Delivering nitric oxide into human skin from encapsulated S-nitrosoglutathione under UV light: An in vitro and ex vivo study

Delivering nitric oxide into human skin from encapsulated S-nitrosoglutathione under UV light: an *in vitro* and *ex vivo* study

Milena T. Pelegrino[1], Richard B. Weller[2], André Paganotti[3], Amedea B. Seabra[1*]

[1]Center for Natural and Human Sciences, Universidade Federal do ABC, Santo André, Brazil.

[2]Medical Research Council Centre for Inflammation Research, University of Edinburgh, Queen's Medical Research Institute.

[3]Laboratory of Materials and Mechanical Manufacture, Universidade Federal de São Paulo, Diadema, Brazil.

[*]E-mail: amedea.seabra@ufabc.edu.br

Abstract

Nitric oxide (NO) is a crucial molecule in the human body. The encapsulation of exogenous NO donors into chitosan nanoparticles (CS NPs) has been widely used to overcome NO drawbacks in pharmacological applications, such as, its short half-life. The NO donor, S-nitrosoglutathione (GSNO), was encapsulated into CS NPs (GSNO-CS NPs) and characterized by AFM and DLS measurements. The nanoparticles presented a hydrodynamic size of 123.3 ± 1.5 nm and a polydispersity of 0.25 ± 0.01. The ability of GSNO-CS NPs, combined with UV irradiation, to deliver NO was evaluated using *ex vivo* human skin. The human skin was pre-treated with GSNO-CS NPs, in the presence and absence of UV irradiation. The results showed that the combined treatment significantly increased the NO and S-nitrosothiol levels in human skin. This effect can emulate the cardiovascular benefits related to NO without negative side effects of skin exposure to UV light.

Keywords: Nitric oxide, S-nitrosothiols, Nanoparticles, Human skin.

1. Introduction

As nitric oxide (NO) is involved in different biological processes [1-9], several strategies have been used to delivery NO in biomedical applications, and in this context, there is a great interest to increase endogenous NO levels [1]. The administration of exogenous NO is limited by its short half-life (seconds), which can restrict the biological reach of NO regarding time, concentration and site [2,3]. There are promising approaches to increase endogenous levels of NO, for examples, the use of delivery systems capable of releasing NO and/or ultraviolet (UV) irradiation [4,5], which might enrich the levels of natural NO storage.

One of the natural storage of NO in the human body is the skin tissue. Human skin can store more stable species of NO, such as nitrite (NO_2^-), nitrate (NO_3^-), and S-nitrosothiols (RSNOs) [6–8]. These NO stores can be decomposed releasing free NO upon UV irradiation such as sun exposure. Once released from the skin, bioactive NO can reach the bloodstream causing the vasodilation of arteries, decreasing peripheral resistance [8], which decreases the arterial blood pressure [9], and thus promoting beneficial effects for the cardiovascular system [8,10].

Another approach to increase the levels of NO *in vivo* is the administration of exogenous materials capable of carrying and delivering NO in a sustainable manner [4,5]. RSNOs are a class of NO donor composed of thiol-containing molecules bound to NO through an S-NO bound, for example, S-nitrosoglutathione (GSNO) [11]. GSNO undergoes a spontaneous decomposition yielding free NO and oxidized glutathione (GS-SG) [12]. This reaction can be catalyzed by light exposure (UV and/or visible light), heat, the presence of copper ions or enzymes [11,12]. Recent progress has been achieved by using topical creams/ointments containing NO donors (such as GSNO), along with a reagent that can accelerate NO release from the RSNOs in the absence of UV light [13]. In this sense, a topical GSNO/Vaseline mixture using a commercial zinc oxide-containing cream was used to topical antimicrobial applications [14]. In a similar approach, ascorbic acid was used to trigger NO decomposition from RSNO-modified NO-releasing chitosan oligosaccharides, as antibacterial agents [15].

Currently available NO donors have several disadvantages, such as the release of NO below the therapeutic range and the instability and/or short duration of action of the NO donor [11]. One approach to the address this drawback is the combination of nanomaterials with NO donors, which has promising implications in pharmacology and biomedical fields [1]. There are several studies from our research group showing the successful incorporation of RSNOs into chitosan nanoparticles (CS NPs) for antimicrobial [16], anticancer [17,18], antiparasitic effects [19,20], and for the promoting NO release in human skin [5].

CS NPs and other chitosan-based materials have been studied as drug-delivery system with enhanced cellular uptake of the encapsulated active drugs [21], for tissue regeneration with major focus on skin [22,23], and for antibacterial treatment [24]. Chitosan (CS) has suitable properties for biomedical and pharmacological applications because of its biocompatibility, biodegradability and mucoadhesive behavior [22]. In addition, the encapsulation of RSNOs into CS NPs promotes a sustained NO release from the NO donor creating a viable material for clinical applications [25].

Since the nineties, there has been an intense and increasing research focused on the investigation of NO roles in the cardiovascular system [8,26–29]. More recently, it has been demonstrated that human skin is an important NO store (NO pool) in the forms of NO_2^-, NO_3^-, and RSNOs that can release NO from the human skin to the bloodstream, under the application of UV light [7,30]. GSNO is the most abundant RSNO found *in vivo* and it undergoes a spontaneous decomposition releasing NO. This reaction can be catalyzed by UV and/or visible irradiation [5,6,8,28,30–36] and indeed, UV irradiation can be used to increase GSNO decomposition and, consequently, increase the rates of NO release [5–8,30,34]. Pelegrino et al. showed that pre-treatment of human skin samples with GSNO-CS NPs under UV exposure increased NO levels in epidermis and dermis layers, as measured by confocal microscopy [5]. However, there is still the need of a systematic and thorough study to better comprehend the interactions between NO donors and UV light.

UV light has negative side effects, such as premature aging and skin cancer. Thus, in this study, we aimed to develop a strategy to increase NO levels in the skin, by applying NO-releasing CS NPs, without greater exposition to UV light, and thus avoiding harmful effects of sunlight. Moreover, in this study, we evaluated the formation of NO and RSNOs in human skin after different wavelength of UV light treatments (290 - 400 nm), combined with skin pre-treatment with CS NPs containing GSNO.

2. Materials and Methods

The effects of the application of different wavelengths of UV light on the formation of NO from GSNO and GSNO-CS NPs was evaluated by *in vitro* analysis in aqueous solutions and in *ex vivo* analysis in skin samples. The GSNO used in this study was synthesized by the nitrosation reaction of glutathione (GSH). The GSNO-CS NPs used were prepared by ionotropic gelation process, followed by the nitrosation of the free thiol group of encapsulated GSH in CS NPs. A single grating monochromator was used to irradiate the aqueous and skin samples with UV light at different wavelengths and energy doses. Human skin samples were acquired from Murrayfield private hospital. The decomposition of free or encapsulated GSNO was measured in the in vitro experiments by using UV-Visible spectrophotometric analysis and the free NO and RSNO levels from treated and untreated skin slices were measured using a nitric oxide electrochemical sensor. More information regarding the chemicals, the GSNO and nanoparticle preparation and characterization are available in the supplementary data published alongside this study.

3. Results and discussion

Firstly, to better comprehend the photochemistry of GSNO in the skin, it is needed to study the photochemistry of GSNO itself. Thus, the results of this study are divided into two sections: the first section aims to evaluate the effects of UV light irradiation, at different wavelengths, in *in vitro* analysis of free and encapsulated GSNO in aqueous solution, and the second section their effects in *ex vivo* skin analyses.

3.1. GSNO decomposition with NO release – *in vitro* analysis

To evaluate the NO release profile generated by free GSNO and GSNO-CS NPs, under UV light irradiation, the solutions (free GSNO or encapsulated GSNO both at 1 mM) were irradiated with monochromatic UV light with varying wavelengths from 260 to 320 nm. For each selected wavelength, the UV-Visible spectra were collected for each solution with varying energy doses from 0 to 10 J/cm². The amount of NO released over time was calculated based on the amount of GSNO decomposition, calculated by Beer-Lambert law at 336 nm, characteristic GSNO absorption band. This data showed that for a same wavelength, the generation of NO presents an initial linear growth and subsequent saturation with the increase of energy dose. As the focus of this study was to analyze the variations in the NO production as a function of the applied irradiation doses, the released NO concentration was normalized by diving it by its maximum saturation value. More details are available at the supplementary data.

Fig. 1-(a) and (b) show the contour maps of generated NO from the decomposition of free GSNO (1.0 mM) , Fig. 1-(a), and GSNO-CS NPs (GSNO concentration of 1.0 mM), Fig. 1-(b). NO concentration is shown in the figure scale. The high levels of NO release from free GSNO and from GSNO-CS NPs were 156.4 - 208.5 µM and 56.0 - 74.7 µM, respectively (colors red to yellow). The moderate levels of NO release from GSNO and GSNO-CS NPs were 78.2 - 156.4 µM and 28.0 - 56.0 µM, respectively (colors green to light blue). In addition, the low levels of NO release from GSNO and GSNO-CS NPs were 0.0 - 78.2 µM and 0.0 - 56.0 µM, respectively (color blue to purple).

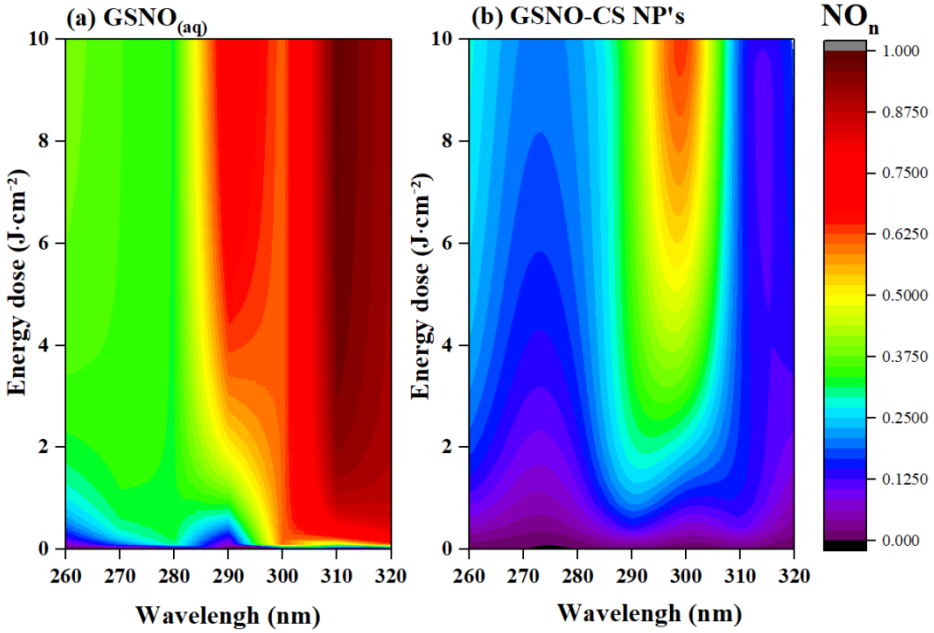

Fig. 1. Contour maps for photochemical NO generated from (A) free GSNO aqueous solution and (B) GSNO-CS NPs under UV irradiation with different wavelengths. In both cases, GSNO concentration was 1.0 mM.

Fig. 1-(a) shows the NO release profile from free and encapsulated GSNO as a function of energy dose, for each tested wavelength ranging from 260 to 320 nm. NO release from aqueous GSNO solution reached a maximum peak at 310 nm that corresponds to 208.5 µM of NO released. High levels of NO (166.8 – 208.5 µM) were generated upon GSNO under irradiation at wavelengths between 290 - 320 nm with amplitude of 30 nm. Under irradiation at 280 nm, NO release was considered moderate (83.4-104.3 µM). Noteworthy, the maximum peak at 310 nm is the same wavelength used for most effective treatment of psoriasis and eczema[37]. This correlation suggests an influence of GSNO decomposition and NO release on psoriasis and eczema treatment.

Fig. 1-(b) shows the NO release from GSNO-CS NPs as a function of energy dose for each tested wavelength ranging from 260 to 320 nm. NO release from GSNO-CS NPs reached a maximum at 300 nm that corresponds to 74.7 µM of NO released. Moreover, high to moderate levels of NO (67.2 – 74.7 µM) were obtained upon GSNO-CS NPs irradiation at 285-305 nm with an amplitude of 20 nm. The intensity of NO release from GSNO-CS NPs was observed to be lower for irradiation at shorter wavelengths (below 285 nm) (7.5 – 14.9 µM) and higher for irradiation with wavelengths longer than 305 nm (7.5 – 14.9 µM).

The incorporation of GSNO into CS NPs decreased the total amount of NO generation and narrowed the spectral window in which NO was released compared to free GSNO. This effect might be related to the UV absorbance peak of CS NPs (see supplementary data), which can protect GSNO from decomposition under UV irradiation. The maximum levels of NO release from free GSNO was 208.5 μM at 310 nm, while for GSNO-CS NPs, the maximum NO release was 74.7 μM at 300 nm. Thus, a *ca*. 2.8-fold higher NO release was observed for free GSNO in comparison with encapsulated GSNO. This result indicates that CS NPs are suitable for the delivery of GSNO, since CS layer might act as a protection barrier, decreasing the rates of GSNO light induced decomposition, in comparison with free GSNO, under the same experimental conditions. Furthermore, it should be noted that the maximum wavelength for NO release from GSNO photodecomposition shifted from 310 to 300 nm upon GSNO incorporation into CS NPs. This effect might be attributed to the incorporation and interactions of GSNO with CS NPs [25]. For a clinical application, not only NO release parameter should be analyzed but the safety ones. It is known in literature that irradiation at 300 nm is much more likely to cause erythema (redness) and DNA damage than 310 nm[37].

Fig. 2 shows the NO release from GSNO and GSNO-CS NPs upon UV irradiation (260 - 320 nm) varying energy doses of 0 - 10 J/cm^2. The dose of applied energy to skin is an important parameter to assess therapy safety. There are currently 225 clinical trials related to light therapy registered in clinicaltrials.gov domain, 72 % of these trials are related to skin diseases treatments. Among several clinical trials, UVA (340 - 400 nm) energy dose was found to be ca. 70-130 J/cm² related to the treatment of scleroderma [38] and for atopic dermatitis treatment [39]. UVB (290 - 320 nm) energy dose was found to be around 0.32 - 4.0 J/cm-², which is related to treatment of dermatoses and keloids [39]. In addition, narrow UVB is the most effective treatment for psoriasis and eczema[37]. Therefore, the energy doses applied in this study can be considered safe for clinical applications and not harmful to skin.

It is important to highlight that the dose of energy applied in different UV ranges has different biological effects [37]. For examples, 1 mJ of irradiation at UVB range causes more DNA damage compared to the same energy dose of irradiation at UVA range [40]. Therefore, to ensure the safety treatment involving UV irradiation, it is important to evaluate the dose energy, as well the UV range [37,40].

The analysis of NO responses to dose (NODR) relates the efficiency of NO release in each applied energy dose as a function of the wavelength. Fig. 2 shows NODR for free GSNO and for GSNO-CS NPs, under irradiation with 260 - 320 nm. The desirable feature is obtained when a low energy dose can generate a high amount of NO from GSNO photodecomposition. Figure 2 shows different profiles of NO photogenerated from free or encapsulated GSNO upon irradiation with different wavelengths. For free GSNO, the curve of NODR as a function of wavelength shows two minimums points, which are centered at 260 and at 290 nm (Fig. 2. In contrast, GSNO-CS NPs have five minimums points centered at 260, 270, 280, 300 and 320 nm (Fig.2). These minimums points indicate that irradiation of the NO donor with this specific wavelength needs high energy to achieve NO photogeneration. Overall, GSNO-CS NPs showed lower

NODR values, in comparison with free GSNO, in all tested wavelength range. This result might be explained by considering the absorbance of light by CS NP layer (see the supplementary data), since encapsulation of GSNO into CS NPs protects the NO donor from photodegradation.

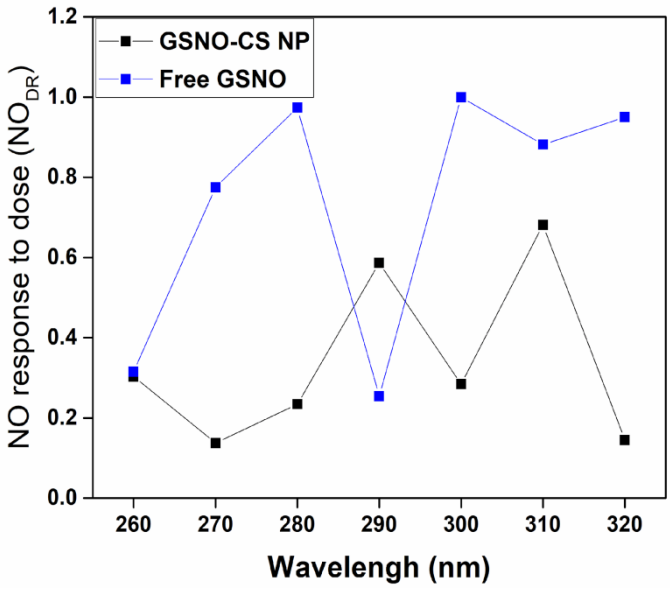

Fig. 2. NO release responses to applied dose of energy (NODR) from free and encapsulated GSNO (1.0 mM) (n=3).

The NODR values reported in this study are in accordance with the literature. The values indicate a high efficiency of NO release in both materials tested and they are expected to have a beneficial effect in a future clinical application. For example, Liu et al. reported a decrease in the blood pressure after 20-30 min of UVA irradiation (320-400 nm at 20 J/cm²), in health volunteers (the energy generated in this application is related to NO generation with high efficiency (NODR ~ 1) [7].

Taken together, UV irradiation triggers NO release from either free or encapsulated GSNO. The NO generation from GSNO and from GSNO-CS NPs has similar maximum peaks at 310 and 300 nm, respectively. The incorporation of GSNO into CS NPs decreases the magnitude of NO release from GSNO-CS NPs, compared to free GSNO, in almost all tested wavelengths.

3.1. GSNO decomposition with NO release – *ex vivo* analysis

Pelegrino et al. showed that pre-treatment of human skin samples with GSNO-CS NPs increased NO levels in epidermis and dermis layers, as measured by confocal microscopy [5]. We have demonstrated that once encapsulated in CS NPs, GSNO diffused from the polymeric matrix to the exterior solution, where the intact GSNO releases free NO by S–N cleavage [14]. In this present work, human skin samples were pre-treated with GSNO-CS NPs (at final GSNO concentration of 100 mM for 2.5 h), in the dark. After this incubation time, the skin samples were twice washed with Milli-Q water and subsequently irradiated at 280 or at 320 nm (3.0 J/cm²). The control group consists of skin samples not pre-treated and not irradiated. After this process, both free NO released and the RSNO levels were measured using the NO meter attached to the

NO electrochemical sensor. We selected two wavelengths, at 280 and at 320 nm, (both at 3.0 J/cm²) to irradiate the skin samples. This selection was based on the fact that irradiation of aqueous solution of GSNO at 280 or at 320 nm led to NO photorelease at moderate (78.2-156.4 μM) and high levels (156.4-208.5 μM), respectively, as shown in Fig. 1. In addition, these two wavelengths (280 and 320 nm) showed superior values of NODR, compared to the values obtained for irradiation with other wavelengths (Fig. 2). In human skin, there are abundant levels of GSNO and other photolabile molecules capable of releasing NO upon irradiation (UV and visible) [5–8,30,34].

Fig. 3 shows that the irradiation of skin samples at both wavelengths (280 and 320 nm) causes an increase in the NO levels, compared to control group (skin in the dark condition). The irradiation of skin samples at 280 nm increased NO levels to an average of 297.3 ± 9.1 pA and irradiation of skin at 320 nm increased NO levels reaching an average of 217.5 ± 45.0 pA. Although the irradiation at 280 nm on free GSNO indicates a high level of NO generation and the irradiation at 320 nm on free GSNO indicates a moderate level of NO generation (Fig. 1), the irradiation at these two wavelengths (280 and 320 nm) showed non-significant differences on human skin. The observed difference between the in vitro experiments with free GSNO solution and ex vivo with human skin samples might be relate to the presence of other photolabile molecules in skin that can affect the formation of intermediary compounds and thus, the final NO release.

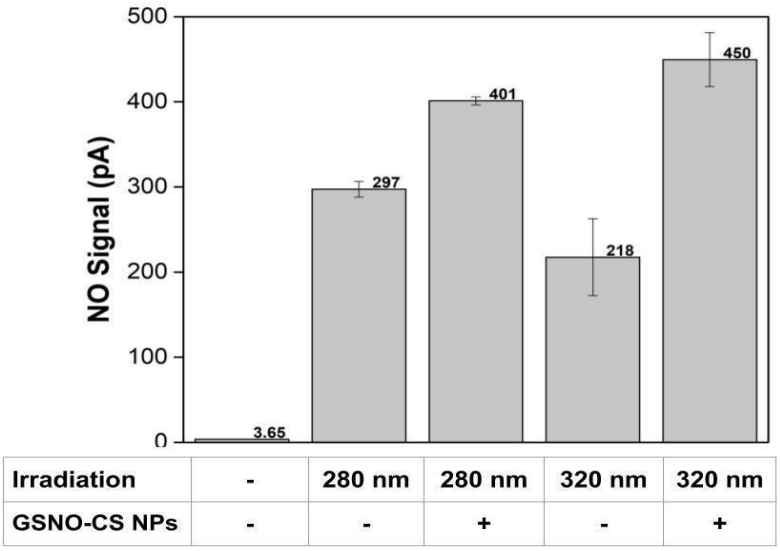

Fig. 3. NO release in human skin after irradiation with 280 and 320 nm (3 J/cm²) and control group (skin in the dark) (n=3).

Moreover, Fig. 3 shows the effects of GSNO-CS NPs pre-treatment on human skin with and without irradiation at 280 or 320 nm (3.0 J/cm²). The NO levels increased after GSNO-CS NPs pre-treatment in both tested irradiation wavelengths (280 or 320 nm), compared with non-pre-treated skin samples. The group pre-treated with GSNO-CS NPs and irradiated at 280 nm has shown an increase of ca. 35% in the level of NO released, compared to the skin irradiated at the same wavelength without pre-treatment with GSNO-CS NPs.

In addition, skin samples pre-treated with GSNO-CS NPs and irradiated at 320 nm have shown an increase of ca. 100 % higher of NO levels, compared to the skin irradiated at the same wavelength without pre-treatment with GSNO-CS NPs (Fig. 3). The GSNO-CS NPs were able to successful delivery NO to human skin samples, increasing the levels of NO in the skin. Thus, the combination of skin irradiation and skin incubation with GSNO-CS NPs further enhanced NO levels reaching almost 2-fold higher values than irradiation alone.

Fig. 4 shows the quantification of RSNO levels on human skin samples after the irradiation at 280 or at 320 nm in the presence and/or absence of skin pre-treatment with GSNO-CS NPs, compared to human skin samples in the dark condition with no pre-treatment. In the absence of pre-treatment, the irradiation of skin at 280 nm was responsible to a 3-fold decrease of RSNO levels, compared to control group (skin in the dark condition). The decrease in RSNOs after skin irradiation might be attributed to RSNO decomposition and NO release. In contrast, irradiation at 320 nm was responsible to 2-fold increase of RSNO levels, compared to control group (light protected skin). Interestingly, these results indicate that skin irradiation with different wavelengths can reduce or increase the levels of RSNOs, in a wavelength dependent fashion. The RSNO formation upon UV irradiation in a biological environment may involve three pathways: (i) oxidation of NO forming peroxynitrite (ONOO-) that undergoes radical recombination that forms nitrogen trioxide (N2O3) which then can nitrosate thiol-containing molecules in biological media; ii) radical recombination, the combination of a thiol radial (RS·) and the NO radial, and (iii) the binding of NO to a transition metal followed by RSNO formation and metal reduction [41–43].

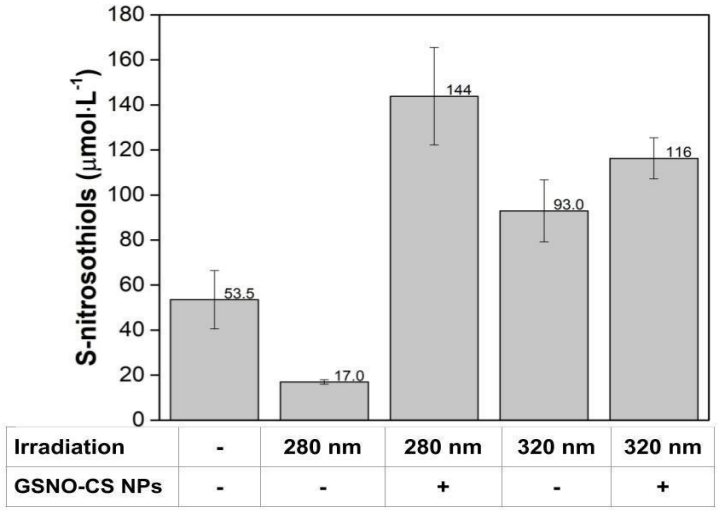

Fig. 4. Concentrations of RSN measured in human skin after irradiation at 280 nm and at 320 nm (3 J/cm²) and for the control group (skin in the dark). The skin samples were pre-incubated with GSNO-CS NPs at 100 mM for 2.5 h at 25 °C (n=3).

In addition, Fig. 4 shows the quantification of RSNO content in human skin samples after pre-treatment with GSNO-CS NPs, with and without irradiation at 280 or 320 nm. The results demonstrated an increase in the levels of RSNO after pre-treatment with GSNO-CS NPs, under UV irradiation at 280 and 320 nm, as expected. The skin group pre-treated with GSNO-CS NPs and irradiated at 280 nm has shown 6-fold higher levels of RSNOs, compared to skin group irradiated at this same wavelength without pre-treatment

with GSNO-CS NPs. Moreover, the skin samples pre-treated with GSNO-CS NPs and irradiated at 320 nm have shown 1.6-fold higher levels of RSNO in the skin, compared to the skin group irradiated at this same wavelength without pre-treatment with GSNO-CS NPs (Fig. 4). Thus, the pre-treatment with GSNO-CS NPs significantly increased the RSNO levels on skin and the combination of GSNO-CS NPs pre-treatment with UV irradiation (at 280 and 320 nm) further increased the RSNO levels on human skin samples.

Overall, the NO levels in human skin samples increased after irradiation at 280 and 320 nm. The skin pre-treatment with GSNO-CS NPs enhanced the NO and RSNO levels compared to irradiation alone. In contrast, the RSNO levels in human skin was increased after irradiation at 320 nm and decreased after 280 nm exposure. To the best of our knowledge, this is the first report to describe the increase and decrease of RSNOs levels in human skin by varying the UV wavelength.

It is well-known that phototherapy, in the visible or near infrared light, has been extensively employed to generate cytotoxic single oxygen that can be allied to the generation of NO from versatile nanomaterials used in different biomedical applications, especially in the combat of cancer cells [44]. For instance, low molecular weight RSNOs can be allied to nanomaterials and photosensitizers to generate NO and single oxygen upon irradiation with near infrared light [45]. Several progresses have been achieved with this NO-phototherapy, mainly against cancer [46]. While visible and near infrared lights have been extensively employed in phototherapy, UV light is considered the major preventable risk factor for skin cancer.

However, recent evidences have demonstrated that sunlight exposure is linked to beneficial effects in the cardiovascular system, since it may lower blood pressure [47]. Human skin contains large stores of nitrogen oxides, and it has been demonstrated that UV light photoreduces these stores to NO, which is exported to the systemic circulation, lowering blood pressure [10]. Sun exposure has been linked to beneficial effects in the cardiovascular system. This effect might be due to an increase of RSNO and NO_2^- levels in human skin [6–8]. It should be noted that irradiation might have negative impacts on health, such as, the increase of skin cancer rates and aging [8,48]. Interestingly, skin treatment with GSNO-CS NPs, in the absence of UV irradiation, might be a new approach to increase NO and RSNO levels in human skin and thus emulate cardiovascular benefits [8], without negative side effects of skin exposure to UV sunlight.

It should be noted that, in practical applications, GSNO-CS NPs allied with light irradiation might find important dermatological applications in the combat of bacterial infection. We have already demonstrated that chitosan and alginate nanoparticles containing low molecular weight RSNOs have important antibacterial effects against *Staphylococcus aureus* and *Escherichia coli* [13]. Moreover, GSNO-containing Pluronic hydrogel showed significant antibacterial effect against *Pseudomonas aeruginos*a [21]. The photo-NO release using nanoparticles has been extensively employed in different biomedical applications, including antibacterial effects. For instance, a photofunctional nanofiber engineered material

able to release NO and single oxygen under illumination with visible light demonstrated antibacterial effects [49]. Recently, photoactivatable microemulsions able to photo-release NO and single oxygen were prepared. The material can operate either individually or in tandem resulting in red, green or both fluorescence emission, photogeneration of cytotoxic NO and single oxygen, and amplified photobactericidal action against *Staphylococcus aureus* [50]. In addition, a patent describes an approach to combat dermatological infections, such as acne, with topical NO delivery system [51]. In this sense, further studies are required to evaluate the potential of GSNO-CS NPs against bacteria, in dermatological applications, associated with light-therapy

Since 1867, organic nitrite in diverse forms has been used in clinical to the treatment of angina pectoris [52]. The first organic nitrate used in clinical was amyl nitrite, which was followed by nitrate nitroglycerin. Despite potent vasodilatory capacity, it is rapidly attenuate by the development of nitrate tolerance [52,53]. Treatment based on nanoparticles delivering NO, without going to nitrate pathways, have an intrinsically advantage compared to currently used drugs. Skin pre-treatment with GSNO-CS NPs could efficiently deliver NO to skin, increase cutaneous RSNO levels and replenish NO reservoirs in the skin. UV irradiation, at specific wavelengths, allied to the topical application of GSNO-CS NPs further increased RSNO levels in human skin, as reported in this work. This increase of NO and RSNO levels in human skin might have positive effects on the cardiovascular system, as previously discussed [6–8,10,30,54,55].

4. Conclusions

The treatment of human skin with GSNO and UV light promoted increased NO release and may also increase cutaneous RSNO stores suggesting a synergetic effect of the UV irradiation and administration of NO donors.

The NO generation from free GSNO or GSNO-CS NPs upon UV irradiation is dependent on the selected UV light wavelength. The peak of NO generation upon UV irradiation from free GSNO or encapsulated GSNO was 310 and 300 nm, respectively. The overall amount of NO generation and wavelength amplitude decreased upon GSNO encapsulation into CS NPs. This may be related to the protection of CS layer against GSNO photodecomposition. This effect can prolong the half-life of GSNO into CS NPs, making them suitable for biomedical applications.

Human skin samples pre-treated with GSNO-CS NPs have significantly increased levels of NO and RSNOs. This effect was further enhanced upon the combination of GSNO-CS NPs and UV irradiation at 280 and at 320 nm. GSNO-CS NPs can deliver NO to human skin, increasing the skin levels of RSNOs, which replenish the the natural NO reservoir in human skin. This effect can reproduce the cardiovascular benefits related to NO without negative side effects of skin exposure to UV light.

Acknowledgements

This work was supported by FAPESP (Procs. 2017/05029-8, 2018/08194-2), CNPq (404815/2018-9), and Newton Advanced Fellowship (The Royal Society NA140046). Multiuser Central Facilities (UFABC) for the experimental support. This study was financed in part by the Coordenação de Aperfeiçoamento de Pessoal de Nível Superior - Brasil (CAPES) - Finance Code 001.

References

[1] A.B. Seabra, G.Z. Justo, P.S. Haddad, State of the art, challenges and perspectives in the design of nitric oxide-releasing polymeric nanomaterials for biomedical applications, Biotechnol. Adv. 33 (2015) 1370–1379. doi:10.1016/j.biotechadv.2015.01.005.

[2] N.S. Bryan, An overview of nitrite and nitrate, in: D. Bagchi (Ed.), Sustain. Energy Enhanc. Hum. Funct. Act., 1st ed., Elsevier, 2017: pp. 53–65. doi:10.1016/B978-0-12-805413-0.00003-X.

[3] Y. Nagasaka, B.O. Fernandez, A.U. Steinbicker, E. Spagnolli, R. Malhotra, D.B. Bloch, K.D. Bloch, W.M. Zapol, M. Feelisch, Pharmacological preconditioning with inhaled nitric oxide (NO): Organ-specific differences in the lifetime of blood and tissue NO metabolites, Nitric Oxide. 80 (2018) 52–60. doi:10.1016/j.niox.2018.08.006.

[4] D.J. Suchyta, M.H. Schoenfisch, Controlled release of nitric oxide from liposomes, ACS Biomater. Sci. Eng. 3 (2017) 2136–2143. doi:10.1021/acsbiomaterials.7b00255.

[5] M.T. Pelegrino, R.B. Weller, X. Chen, J.S. Bernardes, A.B. Seabra, Chitosan nanoparticles for nitric oxide delivery in human skin, Med Chem Comm. 8 (2017) 713–719. doi:10.1039/C6MD00502K.

[6] M. Mowbray, S. McLintock, R. Weerakoon, N. Lomatschinsky, S. Jones, A.G. Rossi, R.B. Weller, Enzyme-independent NO stores in human skin: Quantification and influence of UV radiation, J. Invest. Dermatol. 129 (2009) 834–842. doi:10.1038/jid.2008.296.

[7] D. Liu, B.O. Fernandez, A. Hamilton, N.N. Lang, J.M.C. Gallagher, D.E. Newby, M. Feelisch, R.B. Weller, UVA irradiation of human skin vasodilates arterial vasculature and lowers blood pressure independently of nitric oxide synthase, J. Invest. Dermatol. 134 (2014) 1839–1846. doi:10.1038/jid.2014.27.

[8] R.B. Weller, Sunlight has cardiovascular benefits independently of vitamin D, Blood Purif. 41 (2016) 130–134. doi:10.1159/000441266.

[9] S. Earley, T. Pauyo, R. Drapp, M.J. Tavares, W. Liedtke, J.E. Brayden, TRPV4-dependent dilation of peripheral resistance arteries influences arterial pressure, Am. J. Physiol. Circ. Physiol. 297 (2009) H1096–H1102. doi:10.1152/ajpheart.00241.2009.

[10] F. Wright, R.B. Weller, Risks and benefits of UV radiation in older people: More of a friend than a foe?, Maturitas. 81 (2015) 425–431. doi:10.1016/j.maturitas.2015.05.003.

[11] M.G. de Oliveira, S-Nitrosothiols as platforms for topical nitric oxide delivery, Basic Clin. Pharmacol. Toxicol. 119 (2016) 49–56. doi:10.1111/bcpt.12588.

[12] M.M. Cortese-Krott, B.O. Fernandez, J.L.T. Santos, E. Mergia, M. Grman, P. Nagy, M. Kelm, A. Butler, M. Feelisch, Nitrosopersulfide (SSNO−) accounts for sustained NO bioactivity of S-nitrosothiols following reaction with sulfide, Redox Biol. 2 (2014) 234–244. doi:10.1016/j.redox.2013.12.031.

[13] A.J. Friedman, K. Blecher, D. Schairer, C. Tuckman-Vernon, P. Nacharaju, D. Sanchez, P. Gialanella, L.R. Martinez, J.M. Friedman, J.D. Nosanchuk, Improved antimicrobial efficacy with nitric oxide releasing nanoparticle generated S-nitrosoglutathione, Nitric Oxide. 25 (2011) 381–386. doi:10.1016/j.niox.2011.09.001.

[14] J.C. Doverspike, Y. Zhou, J. Wu, X. Tan, C. Xi, M.E. Meyerhoff, Nitric oxide releasing two-part creams containing S-nitrosoglutathione and zinc oxide for potential topical antimicrobial applications, Nitric Oxide. 90 (2019) 1–9. doi:10.1016/j.niox.2019.05.009.

[15] Y. Lu, A. Shah, R.A. Hunter, R.J. Soto, M.H. Schoenfisch, S -Nitrosothiol-modified nitric oxide-releasing chitosan oligosaccharides as antibacterial agents, Acta Biomater. 12 (2015) 62–69. doi:10.1016/j.actbio.2014.10.028.

[16] V.F. Cardozo, C.A.C. Lancheros, A.M. Narciso, E.C.S. Valereto, R.K.T. Kobayashi, A.B. Seabra, G. Nakazato, Evaluation of antibacterial activity of nitric oxide-releasing polymeric particles against Staphylococcus aureus and Escherichia coli from bovine mastitis, Int. J. Pharm. 473 (2014) 20–29. doi:10.1016/j.ijpharm.2014.06.051.

[17] M.T. Pelegrino, L.C. Silva, C.M. Watashi, P.S. Haddad, T. Rodrigues, A.B. Seabra, Nitric oxide-releasing nanoparticles: synthesis, characterization, and cytotoxicity to tumorigenic cells, J. Nanoparticle Res. 19 (2017) 57. doi:10.1007/s11051-017-3747-4.

[18] L.S. Ferraz, C.M. Watashi, C. Colturato-Kido, M.T. Pelegrino, E.J. Paredes-Gamero, R.B. Weller, A.B. Seabra, T. Rodrigues, Antitumor potential of S -nitrosothiol-containing polymeric nanoparticles against melanoma, Mol. Pharm. 15 (2018) 1160–1168. doi:10.1021/acs.molpharmaceut.7b01001.

[19] A.B. Seabra, N.A. Kitice, M.T. Pelegrino, C.A.C. Lancheros, L.M. Yamauchi, P. Pinge-Filho, S.F. Yamada-Ogatta, Nitric oxide-releasing polymeric nanoparticles against Trypanosoma cruzi, J. Phys. Conf. Ser. 617 (2015) 12020. doi:10.1088/1742-6596/617/1/012020.

[20] C.A.C. Lancheros, M.T. Pelegrino, D. Kian, E.R. Tavares, P.M. Hiraiwa, S. Goldenberg, C.V. Nakamura, L.M. Yamauchi, P. Pinge-Filho, A.B. Seabra, S.F. Yamada-Ogatta, Selective antiprotozoal activity of nitric oxide-releasing chitosan nanoparticles against Trypanosoma cruzi: Toxicity and mechanisms of action, Curr. Pharm. Des. 24 (2018) 830–839. doi:10.2174/1381612824666180209105625.

[21] Q. Wang, Y. Zhao, L. Guan, Y. Zhang, Q. Dang, P. Dong, J. Li, X. Liang, Preparation of astaxanthin-loaded DNA/chitosan nanoparticles for improved cellular uptake and antioxidation capability, Food Chem. 227 (2017) 9–15. doi:10.1016/j.foodchem.2017.01.081.

[22] M. T. Pelegrino, A. B. Seabra, Chitosan-based nanomaterials for skin regeneration, AIMS Med. Sci. 4 (2017) 352–381. doi:10.3934/medsci.2017.3.352.

[23] K. Vig, A. Chaudhari, S. Tripathi, S. Dixit, R. Sahu, S. Pillai, V. Dennis, S. Singh, Advances in skin regeneration using tissue engineering, Int. J. Mol. Sci. 18 (2017) 789. doi:10.3390/ijms18040789.

[24] M. Pelegrino, B.A. Lima, M. do Nascimento, C. Lombello, M. Brocchi, A. Seabra, Biocompatible and antibacterial nitric oxide-releasing pluronic F-127/chitosan hydrogel for topical applications, Polymers (Basel). 10 (2018) 452. doi:10.3390/polym10040452.
[25] M.T. Pelegrino, D.R. de Araújo, A.B. Seabra, S-nitrosoglutathione-containing chitosan nanoparticles dispersed in Pluronic F-127 hydrogel: Potential uses in topical applications, J. Drug Deliv. Sci. Technol. 43 (2018) 211–220. doi:10.1016/j.jddst.2017.10.016.
[26] C.P. Bondonno, X. Yang, K.D. Croft, M.J. Considine, N.C. Ward, L. Rich, I.B. Puddey, E. Swinny, A. Mubarak, J.M. Hodgson, Flavonoid-rich apples and nitrate-rich spinach augment nitric oxide status and improve endothelial function in healthy men and women: a randomized controlled trial, Free Radic. Biol. Med. 52 (2012) 95–102. doi:10.1016/j.freeradbiomed.2011.09.028.
[27] P.M.C. Mommersteeg, R.G. Schoemaker, U.L.M. Eisel, I.M. Garrelds, C.G. Schalkwijk, W.J. Kop, Nitric oxide dysregulation in patients with heart failure, Psychosom. Med. 77 (2015) 292–302. doi:10.1097/PSY.0000000000000162.
[28] A.B. Seabra, M.G. de Oliveira, Poly(vinyl alcohol) and poly(vinyl pyrrolidone) blended films for local nitric oxide release, Biomaterials. 25 (2004) 3773–3782. doi:10.1016/j.biomaterials.2003.10.035.
[29] A.R. Butler, J.H. Ridd, Formation of nitric oxide from nitrous acid in ischemic tissue and skin, Nitric Oxide. 10 (2004) 20–24. doi:10.1016/j.niox.2004.01.004.
[30] C. Opländer, C.M. Volkmar, A. Paunel-Görgülü, E.E. van Faassen, C. Heiss, M. Kelm, D. Halmer, M. Mürtz, N. Pallua, C. V. Suschek, Whole body UVA irradiation lowers systemic blood pressure by release of nitric oxide from intracutaneous photolabile nitric oxide derivates, Circ. Res. 105 (2009) 1031–1040. doi:10.1161/CIRCRESAHA.109.207019.
[31] D.J. Sexton, A. Muruganandam, D.J. McKenney, B. Mutus, Visible light photochemical release of nitric oxide from s-nitrosoglutathione: potential photochemotherapeutic applications, Photochem. Photobiol. 59 (1994) 463–467. doi:10.1111/j.1751-1097.1994.tb05065.x.
[32] J.B. Warren, Nitric oxide and human skin blood flow responses to acetylcholine and ultraviolet light., FASEB J. 8 (1994) 247–251. doi:10.1096/fasebj.8.2.7509761.
[33] S.M. Shishido, A.B. Seabra, W. Loh, M.G. de Oliveira, Thermal and photochemical nitric oxide release from S-nitrosothiols incorporated in Pluronic F127 gel: potential uses for local and controlled nitric oxide release, Biomaterials. 24 (2003) 3543–3553. doi:10.1016/S0142-9612(03)00153-4.
[34] A.N. Paunel, A. Dejam, S. Thelen, M. Kirsch, M. Horstjann, P. Gharini, M. Mürtz, M. Kelm, H. de Groot, V. Kolb-Bachofen, C. V. Suschek, Enzyme-independent nitric oxide formation during UVA challenge of human skin: characterization, molecular sources, and mechanisms, Free Radic. Biol. Med. 38 (2005) 606–615. doi:10.1016/j.freeradbiomed.2004.11.018.
[35] R. Weller, Nitric oxide: a key mediator in cutaneous physiology, Clin. Exp. Dermatol. 28 (2003) 511–514. doi:10.1046/j.1365-2230.2003.01365.x.
[36] R. Zuccarelli, A.C.P. Coelho, L.E.P. Peres, L. Freschi, Shedding light on NO homeostasis: Light as a key regulator of glutathione and nitric oxide metabolisms during seedling deetiolation, Nitric Oxide. 68 (2017) 77–90. doi:10.1016/j.niox.2017.01.006.
[37] A.R. Webb, H. Slaper, P. Koepke, A.W. Schmalwieser, Know your standard: Clarifying the CIE erythema action spectrum, Photochem. Photobiol. 87 (2011) 483–486. doi:10.1111/j.1751-1097.2010.00871.x.
[38] H. Jacobe, Treatment study comparing UVA-1 phototherapy vs placebo treatment for morphea, (2019). https://clinicaltrials.gov/ct2/show/NCT01799174 (accessed July 17, 2019).
[39] J.J. Voorhees, Ultraviolet (UVA and UVB) light therapy in the treatment of inflammatory skin conditions, (2019). https://clinicaltrials.gov/ct2/show/NCT00129415.
[40] A. Gęgotek, P. Domingues, E. Skrzydlewska, Proteins involved in the antioxidant and inflammatory response in rutin-treated human skin fibroblasts exposed to UVA or UVB irradiation, J. Dermatol. Sci. 90 (2018) 241–252. doi:10.1016/j.jdermsci.2018.02.002.
[41] P.C. Ford, I.M. Lorkovic, Mechanistic aspects of the reactions of nitric oxide with transition-metal complexes, Chem. Rev. 102 (2002) 993–1018. doi:10.1021/cr0000271.
[42] B.C. Smith, M.A. Marletta, Mechanisms of S-nitrosothiol formation and selectivity in nitric oxide signaling, Curr. Opin. Chem. Biol. 16 (2012) 498–506. doi:10.1016/j.cbpa.2012.10.016.
[43] S.L. Wynia-Smith, B.C. Smith, Nitrosothiol formation and S-nitrosation signaling through nitric oxide synthases, Nitric Oxide. 63 (2017) 52–60. doi:10.1016/j.niox.2016.10.001.
[44] A. Fraix, S. Sortino, Combination of PDT photosensitizers with NO photodononors, Photochem. Photobiol. Sci. 17 (2018) 1709–1727. doi:10.1039/C8PP00272J.
[45] C. Ratanatawanate, A. Chyao, K.J. Balkus, S- Nitrosocysteine-decorated PbS QDs/TiO2 nanotubes for enhanced production of singlet oxygen, J. Am. Chem. Soc. 133 (2011) 3492–3497. doi:10.1021/ja109328a.
[46] W. Yu, T. Liu, M. Zhang, Z. Wang, J. Ye, C.-X. Li, W. Liu, R. Li, J. Feng, X.-Z. Zhang, O2 economizer for inhibiting cell Respiration to combat the hypoxia obstacle in tumor treatments, ACS Nano. (2019). doi:10.1021/acsnano.8b07852.
[47] R.B. Weller, I love a sunburnt country: there's more to romance than cancer and vitamin D, Wound Rep Reg. 24 (2016) A13–A27.
[48] M.F. Holick, Biological effects of sunlight, ultraviolet radiation, visible light, infrared radiation and vitamin D for health, Anticancer Res. 36 (2016) 1345–1356. doi:0250-7005/2016 $2.00+.40.
[49] J. Dolanský, P. Henke, P. Kubát, A. Fraix, S. Sortino, J. Mosinger, Polystyrene nanofiber materials for visible-light-driven dual antibacterial action via simultaneous photogeneration of NO and O2 (1 Δ g), ACS Appl. Mater. Interfaces. 7 (2015) 22980–22989. doi:10.1021/acsami.5b06233.
[50] A. Fraix, O. Catanzano, I. Di Bari, C. Conte, M. Seggio, C. Parisi, A. Nostro, G. Ginestra, F. Quaglia, S. Sortino, Visible light-activatable multicargo microemulsions with bimodal photobactericidal action and dual colour fluorescence, J. Mater. Chem. B. 7 (2019) 5257–5264. doi:10.1039/C9TB00699K.
[51] N. V. Perricone, C.T. Madison, Systems and methods for treatment of acne vulgaris and other conditions with a topical nitric oxide delivery system, US 2014/0079761 A1, 2014.
[52] T. Münzel, A. Daiber, Inorganic nitrite and nitrate in cardiovascular therapy: A better alternative to organic nitrates as nitric oxide donors?, Vascul. Pharmacol. 102 (2018) 1–10. doi:10.1016/j.vph.2017.11.003.
[53] T. Münzel, A. Daiber, T. Gori, More answers to the still unresolved question of nitrate tolerance, Eur. Heart J. 34 (2013) 2666–2673. doi:10.1093/eurheartj/eht249.
[54] R. Zhang, D.T. Hess, J.D. Reynolds, J.S. Stamler, Hemoglobin S-nitrosylation plays an essential role in cardioprotection, J. Clin. Invest. 126 (2016) 4654–4658. doi:10.1172/JCI90425.
[55] B.K. Alba, J.L. Greaney, S.B. Ferguson, L.M. Alexander, Endothelial function is impaired in the cutaneous microcirculation of adults with psoriasis through reductions in nitric oxide-dependent vasodilation, Am. J. Physiol. Circ. Physiol. 314 (2018) H343–H349. doi:10.1152/ajpheart.00446.2017.

Highlights

- Chitosan nanoparticles (NPs) containing GSNO were synthesized and characterized.
- Chitosan layer protects GSNO from UV decomposition and increases its stability.
- Chitosan nanoparticles loaded with GSNO increased NO and RSNO levels on human skin.
- The combination of NPs and UV radiation further enhances NO and RSNO levels in skin.
- The increase of NO and RSNO levels on skin may decrease blood pressure.

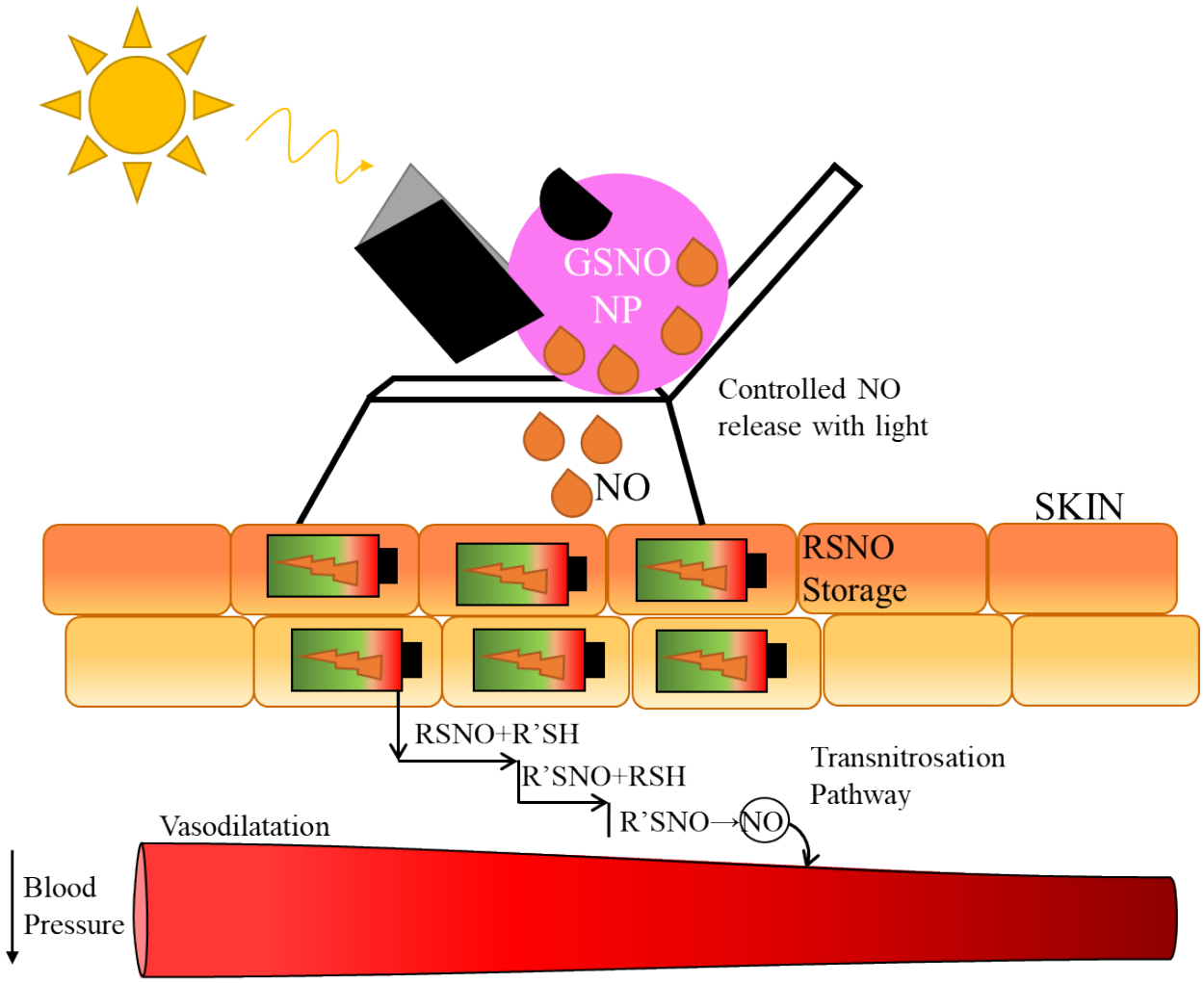
GSNO
NP
Controlled NO
release with light
NO
SKIN
RSNO
Storage
RSNO+R'SH
R'SNO+RSH
R'SNO→NO
Transnitrosation
Pathway
Vasodilatation
Blood
Pressure

Delivering nitric oxide into human skin from encapsulated S-nitrosoglutathione under UV light: an *in vitro* and *ex vivo* study

Milena T. Pelegrino[1], Richard B. Weller[2], André Paganotti[3], Amedea B. Seabra[1*]

[1]Center for Natural and Human Sciences, Universidade Federal do ABC, Santo André, Brazil.

[2]Medical Research Council Centre for Inflammation Research, University of Edinburgh, Queen's Medical Research Institute.

[3]Laboratory of Materials and Mechanical Manufacture, Universidade Federal de São Paulo, Diadema, Brazil.

[*]E-mail: amedea.seabra@ufabc.edu.br

Abstract

Nitric oxide (NO) is a crucial molecule in the human body. The encapsulation of exogenous NO donors into chitosan nanoparticles (CS NPs) has been widely used to overcome NO drawbacks in pharmacological applications, such as, its short half-life. The NO donor, S-nitrosoglutathione (GSNO), was encapsulated into CS NPs (GSNO-CS NPs) and characterized by AFM and DLS measurements. The nanoparticles presented a hydrodynamic size of 123.3 ± 1.5 nm and a polydispersity of 0.25 ± 0.01. The ability of GSNO-CS NPs, combined with UV irradiation, to deliver NO was evaluated using *ex vivo* human skin. The human skin was pre-treated with GSNO-CS NPs, in the presence and absence of UV irradiation. The results showed that the combined treatment significantly increased the NO and S-nitrosothiol levels in human skin. This effect can emulate the cardiovascular benefits related to NO without negative side effects of skin exposure to UV light.

Keywords: Nitric oxide, S-nitrosothiols, Nanoparticles, Human skin.

1. Introduction

As nitric oxide (NO) is involved in different biological processes [1-9], several strategies have been used to delivery NO in biomedical applications, and in this context, there is a great interest to increase endogenous NO levels [1]. The administration of exogenous NO is limited by its short half-life (seconds), which can restrict the biological reach of NO regarding time, concentration and site [2,3]. There are promising approaches to increase endogenous levels of NO, for examples, the use of delivery systems capable of releasing NO and/or ultraviolet (UV) irradiation [4,5], which might enrich the levels of natural NO storage.

One of the natural storage of NO in the human body is the skin tissue. Human skin can store more stable species of NO, such as nitrite (NO_2^-), nitrate (NO_3^-), and S-nitrosothiols (RSNOs) [6–8]. These NO stores can be decomposed releasing free NO upon UV irradiation such as sun exposure. Once released from the skin, bioactive NO can reach the bloodstream causing the vasodilation of arteries, decreasing peripheral resistance [8], which decreases the arterial blood pressure [9], and thus promoting beneficial effects for the cardiovascular system [8,10].

Another approach to increase the levels of NO *in vivo* is the administration of exogenous materials capable of carrying and delivering NO in a sustainable manner [4,5]. RSNOs are a class of NO donor

composed of thiol-containing molecules bound to NO through an S-NO bound, for example, S-nitrosoglutathione (GSNO) [11]. GSNO undergoes a spontaneous decomposition yielding free NO and oxidized glutathione (GS-SG) [12]. This reaction can be catalyzed by light exposure (UV and/or visible light), heat, the presence of copper ions or enzymes [11,12]. Recent progress has been achieved by using topical creams/ointments containing NO donors (such as GSNO), along with a reagent that can accelerate NO release from the RSNOs in the absence of UV light [13]. In this sense, a topical GSNO/Vaseline mixture using a commercial zinc oxide-containing cream was used to topical antimicrobial applications [14]. In a similar approach, ascorbic acid was used to trigger NO decomposition from RSNO-modified NO-releasing chitosan oligosaccharides, as antibacterial agents [15].

Currently available NO donors have several disadvantages, such as the release of NO below the therapeutic range and the instability and/or short duration of action of the NO donor [11]. One approach to the address this drawback is the combination of nanomaterials with NO donors, which has promising implications in pharmacology and biomedical fields [1]. There are several studies from our research group showing the successful incorporation of RSNOs into chitosan nanoparticles (CS NPs) for antimicrobial [16], anticancer [17,18], antiparasitic effects [19,20], and for the promoting NO release in human skin [5].

CS NPs and other chitosan-based materials have been studied as drug-delivery system with enhanced cellular uptake of the encapsulated active drugs [21], for tissue regeneration with major focus on skin [22,23], and for antibacterial treatment [24]. Chitosan (CS) has suitable properties for biomedical and pharmacological applications because of its biocompatibility, biodegradability and mucoadhesive behavior [22]. In addition, the encapsulation of RSNOs into CS NPs promotes a sustained NO release from the NO donor creating a viable material for clinical applications [25].

Since the nineties, there has been an intense and increasing research focused on the investigation of NO roles in the cardiovascular system [8,26–29]. More recently, it has been demonstrated that human skin is an important NO store (NO pool) in the forms of NO_2^-, NO_3^-, and RSNOs that can release NO from the human skin to the bloodstream, under the application of UV light [7,30]. GSNO is the most abundant RSNO found *in vivo* and it undergoes a spontaneous decomposition releasing NO. This reaction can be catalyzed by UV and/or visible irradiation [5,6,8,28,30–36] and indeed, UV irradiation can be used to increase GSNO decomposition and, consequently, increase the rates of NO release [5–8,30,34]. Pelegrino et al. showed that pre-treatment of human skin samples with GSNO-CS NPs under UV exposure increased NO levels in epidermis and dermis layers, as measured by confocal microscopy [5]. However, there is still the need of a systematic and thorough study to better comprehend the interactions between NO donors and UV light.

UV light has negative side effects, such as premature aging and skin cancer. Thus, in this study, we aimed to develop a strategy to increase NO levels in the skin, by applying NO-releasing CS NPs, without greater exposition to UV light, and thus avoiding harmful effects of sunlight. Moreover, in this study, we

evaluated the formation of NO and RSNOs in human skin after different wavelength of UV light treatments (290 - 400 nm), combined with skin pre-treatment with CS NPs containing GSNO.

2. Materials and Methods

The effects of the application of different wavelengths of UV light on the formation of NO from GSNO and GSNO-CS NPs was evaluated by *in vitro* analysis in aqueous solutions and in *ex vivo* analysis in skin samples. The GSNO used in this study was synthesized by the nitrosation reaction of glutathione (GSH). The GSNO-CS NPs used were prepared by ionotropic gelation process, followed by the nitrosation of the free thiol group of encapsulated GSH in CS NPs. A single grating monochromator was used to irradiate the aqueous and skin samples with UV light at different wavelengths and energy doses. Human skin samples were acquired from Murrayfield private hospital. The decomposition of free or encapsulated GSNO was measured in the in vitro experiments by using UV-Visible spectrophotometric analysis and the free NO and RSNO levels from treated and untreated skin slices were measured using a nitric oxide electrochemical sensor. More information regarding the chemicals, the GSNO and nanoparticle preparation and characterization are available in the supplementary data published alongside this study.

3. Results and discussion

Firstly, to better comprehend the photochemistry of GSNO in the skin, it is needed to study the photochemistry of GSNO itself. Thus, the results of this study are divided into two sections: the first section aims to evaluate the effects of UV light irradiation, at different wavelengths, in *in vitro* analysis of free and encapsulated GSNO in aqueous solution, and the second section their effects in *ex vivo* skin analyses.

3.1. GSNO decomposition with NO release – *in vitro* analysis

To evaluate the NO release profile generated by free GSNO and GSNO-CS NPs, under UV light irradiation, the solutions (free GSNO or encapsulated GSNO both at 1 mM) were irradiated with monochromatic UV light with varying wavelengths from 260 to 320 nm. For each selected wavelength, the UV-Visible spectra were collected for each solution with varying energy doses from 0 to 10 J/cm². The amount of NO released over time was calculated based on the amount of GSNO decomposition, calculated by Beer-Lambert law at 336 nm, characteristic GSNO absorption band. This data showed that for a same wavelength, the generation of NO presents an initial linear growth and subsequent saturation with the increase of energy dose. As the focus of this study was to analyze the variations in the NO production as a function of the applied irradiation doses, the released NO concentration was normalized by diving it by its maximum saturation value. More details are available at the supplementary data.

Fig. 1-(a) and (b) show the contour maps of generated NO from the decomposition of free GSNO (1.0 mM) , Fig. 1-(a), and GSNO-CS NPs (GSNO concentration of 1.0 mM), Fig. 1-(b). NO concentration is shown in the figure scale. The high levels of NO release from free GSNO and from GSNO-CS NPs were 156.4 -

208.5 µM and 56.0 - 74.7 µM, respectively (colors red to yellow). The moderate levels of NO release from GSNO and GSNO-CS NPs were 78.2 - 156.4 µM and 28.0 - 56.0 µM, respectively (colors green to light blue). In addition, the low levels of NO release from GSNO and GSNO-CS NPs were 0.0 - 78.2 µM and 0.0 - 56.0 µM, respectively (color blue to purple).

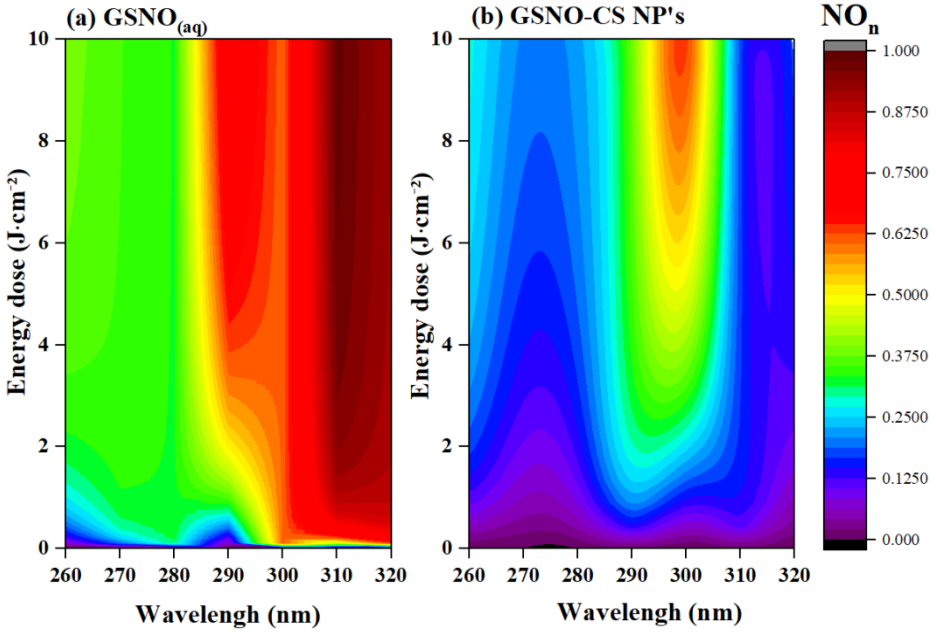

Fig. 1. Contour maps for photochemical NO generated from (A) free GSNO aqueous solution and (B) GSNO-CS NPs under UV irradiation with different wavelengths. In both cases, GSNO concentration was 1.0 mM.

Fig. 1-(a) shows the NO release profile from free and encapsulated GSNO as a function of energy dose, for each tested wavelength ranging from 260 to 320 nm. NO release from aqueous GSNO solution reached a maximum peak at 310 nm that corresponds to 208.5 µM of NO released. High levels of NO (166.8 – 208.5 µM) were generated upon GSNO under irradiation at wavelengths between 290 - 320 nm with amplitude of 30 nm. Under irradiation at 280 nm, NO release was considered moderate (83.4-104.3 µM). Noteworthy, the maximum peak at 310 nm is the same wavelength used for most effective treatment of psoriasis and eczema[37]. This correlation suggests an influence of GSNO decomposition and NO release on psoriasis and eczema treatment.

Fig. 1-(b) shows the NO release from GSNO-CS NPs as a function of energy dose for each tested wavelength ranging from 260 to 320 nm. NO release from GSNO-CS NPs reached a maximum at 300 nm that corresponds to 74.7 µM of NO released. Moreover, high to moderate levels of NO (67.2 – 74.7 µM) were obtained upon GSNO-CS NPs irradiation at 285-305 nm with an amplitude of 20 nm. The intensity of NO release from GSNO-CS NPs was observed to be lower for irradiation at shorter wavelengths (below 285 nm) (7.5 – 14.9 µM) and higher for irradiation with wavelengths longer than 305 nm (7.5 – 14.9 µM).

The incorporation of GSNO into CS NPs decreased the total amount of NO generation and narrowed the spectral window in which NO was released compared to free GSNO. This effect might be related to the UV absorbance peak of CS NPs (see supplementary data), which can protect GSNO from decomposition under

UV irradiation. The maximum levels of NO release from free GSNO was 208.5 μM at 310 nm, while for GSNO-CS NPs, the maximum NO release was 74.7 μM at 300 nm. Thus, a *ca*. 2.8-fold higher NO release was observed for free GSNO in comparison with encapsulated GSNO. This result indicates that CS NPs are suitable for the delivery of GSNO, since CS layer might act as a protection barrier, decreasing the rates of GSNO light induced decomposition, in comparison with free GSNO, under the same experimental conditions. Furthermore, it should be noted that the maximum wavelength for NO release from GSNO photodecomposition shifted from 310 to 300 nm upon GSNO incorporation into CS NPs. This effect might be attributed to the incorporation and interactions of GSNO with CS NPs [25]. For a clinical application, not only NO release parameter should be analyzed but the safety ones. It is known in literature that irradiation at 300 nm is much more likely to cause erythema (redness) and DNA damage than 310 nm[37].

Fig. 2 shows the NO release from GSNO and GSNO-CS NPs upon UV irradiation (260 - 320 nm) varying energy doses of 0 - 10 J/cm^2. The dose of applied energy to skin is an important parameter to assess therapy safety. There are currently 225 clinical trials related to light therapy registered in clinicaltrials.gov domain, 72 % of these trials are related to skin diseases treatments. Among several clinical trials, UVA (340 - 400 nm) energy dose was found to be ca. 70-130 J/cm² related to the treatment of scleroderma [38] and for atopic dermatitis treatment [39]. UVB (290 - 320 nm) energy dose was found to be around 0.32 - 4.0 J/cm-², which is related to treatment of dermatoses and keloids [39]. In addition, narrow UVB is the most effective treatment for psoriasis and eczema[37]. Therefore, the energy doses applied in this study can be considered safe for clinical applications and not harmful to skin.

It is important to highlight that the dose of energy applied in different UV ranges has different biological effects [37]. For examples, 1 mJ of irradiation at UVB range causes more DNA damage compared to the same energy dose of irradiation at UVA range [40]. Therefore, to ensure the safety treatment involving UV irradiation, it is important to evaluate the dose energy, as well the UV range [37,40].

The analysis of NO responses to dose (NODR) relates the efficiency of NO release in each applied energy dose as a function of the wavelength. Fig. 2 shows NODR for free GSNO and for GSNO-CS NPs, under irradiation with 260 - 320 nm. The desirable feature is obtained when a low energy dose can generate a high amount of NO from GSNO photodecomposition. Figure 2 shows different profiles of NO photogenerated from free or encapsulated GSNO upon irradiation with different wavelengths. For free GSNO, the curve of NODR as a function of wavelength shows two minimums points, which are centered at 260 and at 290 nm (Fig. 2. In contrast, GSNO-CS NPs have five minimums points centered at 260, 270, 280, 300 and 320 nm (Fig.2). These minimums points indicate that irradiation of the NO donor with this specific wavelength needs high energy to achieve NO photogeneration. Overall, GSNO-CS NPs showed lower NODR values, in comparison with free GSNO, in all tested wavelength range. This result might be explained by considering the absorbance of light by CS NP layer (see the supplementary data), since encapsulation of GSNO into CS NPs protects the NO donor from photodegradation.

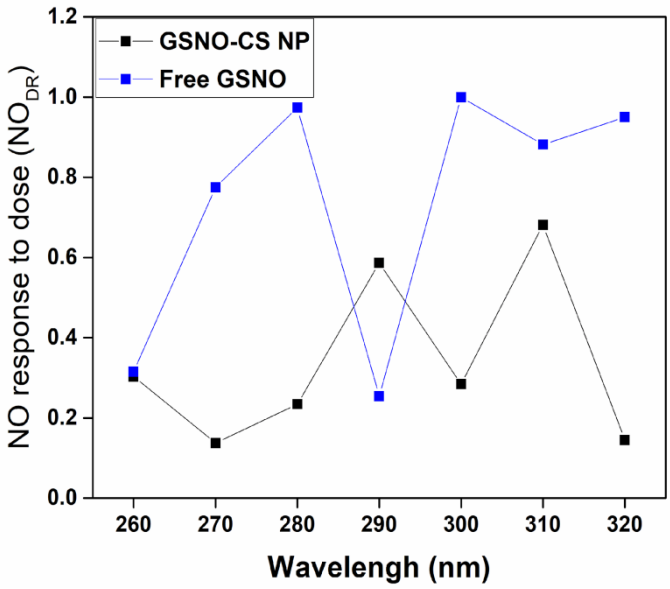

Fig. 2. NO release responses to applied dose of energy (NODR) from free and encapsulated GSNO (1.0 mM) (n=3).

The NODR values reported in this study are in accordance with the literature. The values indicate a high efficiency of NO release in both materials tested and they are expected to have a beneficial effect in a future clinical application. For example, Liu et al. reported a decrease in the blood pressure after 20-30 min of UVA irradiation (320-400 nm at 20 J/cm²), in health volunteers (the energy generated in this application is related to NO generation with high efficiency (NODR ~ 1) [7].

Taken together, UV irradiation triggers NO release from either free or encapsulated GSNO. The NO generation from GSNO and from GSNO-CS NPs has similar maximum peaks at 310 and 300 nm, respectively. The incorporation of GSNO into CS NPs decreases the magnitude of NO release from GSNO-CS NPs, compared to free GSNO, in almost all tested wavelengths.

3.1. GSNO decomposition with NO release – *ex vivo* analysis

Pelegrino et al. showed that pre-treatment of human skin samples with GSNO-CS NPs increased NO levels in epidermis and dermis layers, as measured by confocal microscopy [5]. We have demonstrated that once encapsulated in CS NPs, GSNO diffused from the polymeric matrix to the exterior solution, where the intact GSNO releases free NO by S–N cleavage [14]. In this present work, human skin samples were pre-treated with GSNO-CS NPs (at final GSNO concentration of 100 mM for 2.5 h), in the dark. After this incubation time, the skin samples were twice washed with Milli-Q water and subsequently irradiated at 280 or at 320 nm (3.0 J/cm²). The control group consists of skin samples not pre-treated and not irradiated. After this process, both free NO released and the RSNO levels were measured using the NO meter attached to the NO electrochemical sensor. We selected two wavelengths, at 280 and at 320 nm, (both at 3.0 J/cm²) to irradiate the skin samples. This selection was based on the fact that irradiation of aqueous solution of GSNO at 280 or at 320 nm led to NO photorelease at moderate (78.2-156.4 μM) and high levels (156.4-208.5 μM), respectively, as shown in Fig. 1. In addition, these two wavelengths (280 and 320 nm) showed superior values

of NODR, compared to the values obtained for irradiation with other wavelengths (Fig. 2). In human skin, there are abundant levels of GSNO and other photolabile molecules capable of releasing NO upon irradiation (UV and visible) [5–8,30,34].

Fig. 3 shows that the irradiation of skin samples at both wavelengths (280 and 320 nm) causes an increase in the NO levels, compared to control group (skin in the dark condition). The irradiation of skin samples at 280 nm increased NO levels to an average of 297.3 ± 9.1 pA and irradiation of skin at 320 nm increased NO levels reaching an average of 217.5 ± 45.0 pA. Although the irradiation at 280 nm on free GSNO indicates a high level of NO generation and the irradiation at 320 nm on free GSNO indicates a moderate level of NO generation (Fig. 1), the irradiation at these two wavelengths (280 and 320 nm) showed non-significant differences on human skin. The observed difference between the in vitro experiments with free GSNO solution and ex vivo with human skin samples might be relate to the presence of other photolabile molecules in skin that can affect the formation of intermediary compounds and thus, the final NO release.

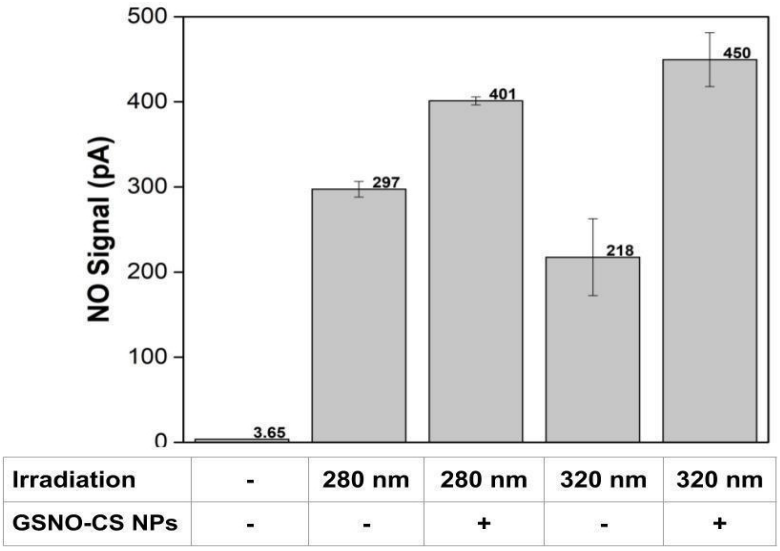

Fig. 3. NO release in human skin after irradiation with 280 and 320 nm (3 J/cm²) and control group (skin in the dark) (n=3).

Moreover, Fig. 3 shows the effects of GSNO-CS NPs pre-treatment on human skin with and without irradiation at 280 or 320 nm (3.0 J/cm²). The NO levels increased after GSNO-CS NPs pre-treatment in both tested irradiation wavelengths (280 or 320 nm), compared with non-pre-treated skin samples. The group pre-treated with GSNO-CS NPs and irradiated at 280 nm has shown an increase of ca. 35% in the level of NO released, compared to the skin irradiated at the same wavelength without pre-treatment with GSNO-CS NPs. In addition, skin samples pre-treated with GSNO-CS NPs and irradiated at 320 nm have shown an increase of ca. 100 % higher of NO levels, compared to the skin irradiated at the same wavelength without pre-treatment with GSNO-CS NPs (Fig. 3). The GSNO-CS NPs were able to successful delivery NO to human skin samples, increasing the levels of NO in the skin. Thus, the combination of skin irradiation and skin incubation with GSNO-CS NPs further enhanced NO levels reaching almost 2-fold higher values than irradiation alone.

Fig. 4 shows the quantification of RSNO levels on human skin samples after the irradiation at 280 or at 320 nm in the presence and/or absence of skin pre-treatment with GSNO-CS NPs, compared to human skin samples in the dark condition with no pre-treatment. In the absence of pre-treatment, the irradiation of skin at 280 nm was responsible to a 3-fold decrease of RSNO levels, compared to control group (skin in the dark condition). The decrease in RSNOs after skin irradiation might be attributed to RSNO decomposition and NO release. In contrast, irradiation at 320 nm was responsible to 2-fold increase of RSNO levels, compared to control group (light protected skin). Interestingly, these results indicate that skin irradiation with different wavelengths can reduce or increase the levels of RSNOs, in a wavelength dependent fashion. The RSNO formation upon UV irradiation in a biological environment may involve three pathways: (i) oxidation of NO forming peroxynitrite (ONOO-) that undergoes radical recombination that forms nitrogen trioxide (N2O3) which then can nitrosate thiol-containing molecules in biological media; ii) radical recombination, the combination of a thiol radial (RS·) and the NO radial, and (iii) the binding of NO to a transition metal followed by RSNO formation and metal reduction [41–43].

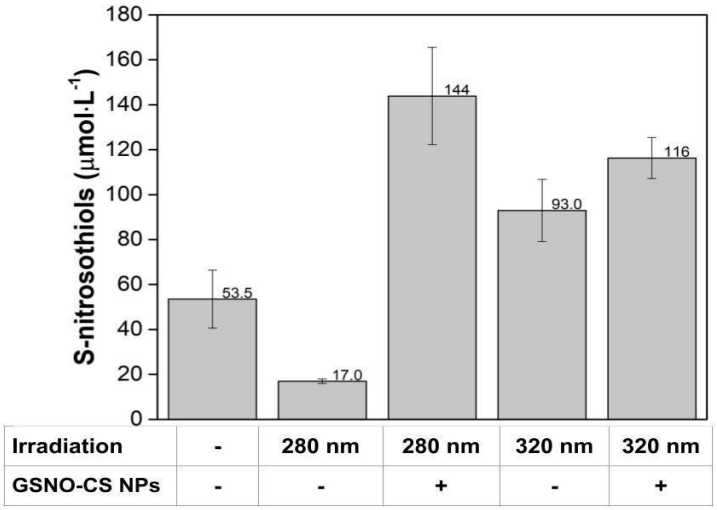

Fig. 4. Concentrations of RSN measured in human skin after irradiation at 280 nm and at 320 nm (3 J/cm²) and for the control group (skin in the dark). The skin samples were pre-incubated with GSNO-CS NPs at 100 mM for 2.5 h at 25 °C (n=3).

In addition, Fig. 4 shows the quantification of RSNO content in human skin samples after pre-treatment with GSNO-CS NPs, with and without irradiation at 280 or 320 nm. The results demonstrated an increase in the levels of RSNO after pre-treatment with GSNO-CS NPs, under UV irradiation at 280 and 320 nm, as expected. The skin group pre-treated with GSNO-CS NPs and irradiated at 280 nm has shown 6-fold higher levels of RSNOs, compared to skin group irradiated at this same wavelength without pre-treatment with GSNO-CS NPs. Moreover, the skin samples pre-treated with GSNO-CS NPs and irradiated at 320 nm have shown 1.6-fold higher levels of RSNO in the skin, compared to the skin group irradiated at this same wavelength without pre-treatment with GSNO-CS NPs (Fig. 4). Thus, the pre-treatment with GSNO-CS NPs significantly increased the RSNO levels on skin and the combination of GSNO-CS NPs pre-treatment with UV irradiation (at 280 and 320 nm) further increased the RSNO levels on human skin samples.

Overall, the NO levels in human skin samples increased after irradiation at 280 and 320 nm. The skin pre-treatment with GSNO-CS NPs enhanced the NO and RSNO levels compared to irradiation alone. In contrast, the RSNO levels in human skin was increased after irradiation at 320 nm and decreased after 280 nm exposure. To the best of our knowledge, this is the first report to describe the increase and decrease of RSNOs levels in human skin by varying the UV wavelength.

It is well-known that phototherapy, in the visible or near infrared light, has been extensively employed to generate cytotoxic single oxygen that can be allied to the generation of NO from versatile nanomaterials used in different biomedical applications, especially in the combat of cancer cells [44]. For instance, low molecular weight RSNOs can be allied to nanomaterials and photosensitizers to generate NO and single oxygen upon irradiation with near infrared light [45]. Several progresses have been achieved with this NO-phototherapy, mainly against cancer [46]. While visible and near infrared lights have been extensively employed in phototherapy, UV light is considered the major preventable risk factor for skin cancer.

However, recent evidences have demonstrated that sunlight exposure is linked to beneficial effects in the cardiovascular system, since it may lower blood pressure [47]. Human skin contains large stores of nitrogen oxides, and it has been demonstrated that UV light photoreduces these stores to NO, which is exported to the systemic circulation, lowering blood pressure [10]. Sun exposure has been linked to beneficial effects in the cardiovascular system. This effect might be due to an increase of RSNO and NO_2^- levels in human skin [6–8]. It should be noted that irradiation might have negative impacts on health, such as, the increase of skin cancer rates and aging [8,48]. Interestingly, skin treatment with GSNO-CS NPs, in the absence of UV irradiation, might be a new approach to increase NO and RSNO levels in human skin and thus emulate cardiovascular benefits [8], without negative side effects of skin exposure to UV sunlight.

It should be noted that, in practical applications, GSNO-CS NPs allied with light irradiation might find important dermatological applications in the combat of bacterial infection. We have already demonstrated that chitosan and alginate nanoparticles containing low molecular weight RSNOs have important antibacterial effects against *Staphylococcus aureus* and *Escherichia coli* [13]. Moreover, GSNO-containing Pluronic hydrogel showed significant antibacterial effect against *Pseudomonas aeruginos*a [21]. The photo-NO release using nanoparticles has been extensively employed in different biomedical applications, including antibacterial effects. For instance, a photofunctional nanofiber engineered material able to release NO and single oxygen under illumination with visible light demonstrated antibacterial effects [49]. Recently, photoactivatable microemulsions able to photo-release NO and single oxygen were prepared. The material can operate either individually or in tandem resulting in red, green or both fluorescence emission, photogeneration of cytotoxic NO and single oxygen, and amplified photobactericidal action against *Staphylococcus aureus* [50]. In addition, a patent describes an approach to combat dermatological infections, such as acne, with topical NO delivery system [51]. In this sense, further studies are required to evaluate the potential of GSNO-CS NPs against bacteria, in dermatological applications, associated with light-therapy

Since 1867, organic nitrite in diverse forms has been used in clinical to the treatment of angina pectoris [52]. The first organic nitrate used in clinical was amyl nitrite, which was followed by nitrate nitroglycerin. Despite potent vasodilatory capacity, it is rapidly attenuate by the development of nitrate tolerance [52,53]. Treatment based on nanoparticles delivering NO, without going to nitrate pathways, have an intrinsically advantage compared to currently used drugs. Skin pre-treatment with GSNO-CS NPs could efficiently deliver NO to skin, increase cutaneous RSNO levels and replenish NO reservoirs in the skin. UV irradiation, at specific wavelengths, allied to the topical application of GSNO-CS NPs further increased RSNO levels in human skin, as reported in this work. This increase of NO and RSNO levels in human skin might have positive effects on the cardiovascular system, as previously discussed [6–8,10,30,54,55].

4. Conclusions

The treatment of human skin with GSNO and UV light promoted increased NO release and may also increase cutaneous RSNO stores suggesting a synergetic effect of the UV irradiation and administration of NO donors.

The NO generation from free GSNO or GSNO-CS NPs upon UV irradiation is dependent on the selected UV light wavelength. The peak of NO generation upon UV irradiation from free GSNO or encapsulated GSNO was 310 and 300 nm, respectively. The overall amount of NO generation and wavelength amplitude decreased upon GSNO encapsulation into CS NPs. This may be related to the protection of CS layer against GSNO photodecomposition. This effect can prolong the half-life of GSNO into CS NPs, making them suitable for biomedical applications.

Human skin samples pre-treated with GSNO-CS NPs have significantly increased levels of NO and RSNOs. This effect was further enhanced upon the combination of GSNO-CS NPs and UV irradiation at 280 and at 320 nm. GSNO-CS NPs can deliver NO to human skin, increasing the skin levels of RSNOs, which replenish the the natural NO reservoir in human skin. This effect can reproduce the cardiovascular benefits related to NO without negative side effects of skin exposure to UV light.

Acknowledgements

This work was supported by FAPESP (Procs. 2017/05029-8, 2018/08194-2), CNPq (404815/2018-9), and Newton Advanced Fellowship (The Royal Society NA140046). Multiuser Central Facilities (UFABC) for the experimental support. This study was financed in part by the Coordenação de Aperfeiçoamento de Pessoal de Nível Superior - Brasil (CAPES) - Finance Code 001.

References

[1] A.B. Seabra, G.Z. Justo, P.S. Haddad, State of the art, challenges and perspectives in the design of nitric oxide-releasing polymeric nanomaterials for biomedical applications, Biotechnol. Adv. 33 (2015) 1370–1379. doi:10.1016/j.biotechadv.2015.01.005.

[2] N.S. Bryan, An overview of nitrite and nitrate, in: D. Bagchi (Ed.), Sustain. Energy Enhanc. Hum. Funct. Act., 1st ed., Elsevier, 2017:

pp. 53–65. doi:10.1016/B978-0-12-805413-0.00003-X.
[3] Y. Nagasaka, B.O. Fernandez, A.U. Steinbicker, E. Spagnolli, R. Malhotra, D.B. Bloch, K.D. Bloch, W.M. Zapol, M. Feelisch, Pharmacological preconditioning with inhaled nitric oxide (NO): Organ-specific differences in the lifetime of blood and tissue NO metabolites, Nitric Oxide. 80 (2018) 52–60. doi:10.1016/j.niox.2018.08.006.
[4] D.J. Suchyta, M.H. Schoenfisch, Controlled release of nitric oxide from liposomes, ACS Biomater. Sci. Eng. 3 (2017) 2136–2143. doi:10.1021/acsbiomaterials.7b00255.
[5] M.T. Pelegrino, R.B. Weller, X. Chen, J.S. Bernardes, A.B. Seabra, Chitosan nanoparticles for nitric oxide delivery in human skin, Med Chem Comm. 8 (2017) 713–719. doi:10.1039/C6MD00502K.
[6] M. Mowbray, S. McLintock, R. Weerakoon, N. Lomatschinsky, S. Jones, A.G. Rossi, R.B. Weller, Enzyme-independent NO stores in human skin: Quantification and influence of UV radiation, J. Invest. Dermatol. 129 (2009) 834–842. doi:10.1038/jid.2008.296.
[7] D. Liu, B.O. Fernandez, A. Hamilton, N.N. Lang, J.M.C. Gallagher, D.E. Newby, M. Feelisch, R.B. Weller, UVA irradiation of human skin vasodilates arterial vasculature and lowers blood pressure independently of nitric oxide synthase, J. Invest. Dermatol. 134 (2014) 1839–1846. doi:10.1038/jid.2014.27.
[8] R.B. Weller, Sunlight has cardiovascular benefits independently of vitamin D, Blood Purif. 41 (2016) 130–134. doi:10.1159/000441266.
[9] S. Earley, T. Pauyo, R. Drapp, M.J. Tavares, W. Liedtke, J.E. Brayden, TRPV4-dependent dilation of peripheral resistance arteries influences arterial pressure, Am. J. Physiol. Circ. Physiol. 297 (2009) H1096–H1102. doi:10.1152/ajpheart.00241.2009.
[10] F. Wright, R.B. Weller, Risks and benefits of UV radiation in older people: More of a friend than a foe?, Maturitas. 81 (2015) 425–431. doi:10.1016/j.maturitas.2015.05.003.
[11] M.G. de Oliveira, S-Nitrosothiols as platforms for topical nitric oxide delivery, Basic Clin. Pharmacol. Toxicol. 119 (2016) 49–56. doi:10.1111/bcpt.12588.
[12] M.M. Cortese-Krott, B.O. Fernandez, J.L.T. Santos, E. Mergia, M. Grman, P. Nagy, M. Kelm, A. Butler, M. Feelisch, Nitrosopersulfide (SSNO−) accounts for sustained NO bioactivity of S-nitrosothiols following reaction with sulfide, Redox Biol. 2 (2014) 234–244. doi:10.1016/j.redox.2013.12.031.
[13] A.J. Friedman, K. Blecher, D. Schairer, C. Tuckman-Vernon, P. Nacharaju, D. Sanchez, P. Gialanella, L.R. Martinez, J.M. Friedman, J.D. Nosanchuk, Improved antimicrobial efficacy with nitric oxide releasing nanoparticle generated S-nitrosoglutathione, Nitric Oxide. 25 (2011) 381–386. doi:10.1016/j.niox.2011.09.001.
[14] J.C. Doverspike, Y. Zhou, J. Wu, X. Tan, C. Xi, M.E. Meyerhoff, Nitric oxide releasing two-part creams containing S-nitrosoglutathione and zinc oxide for potential topical antimicrobial applications, Nitric Oxide. 90 (2019) 1–9. doi:10.1016/j.niox.2019.05.009.
[15] Y. Lu, A. Shah, R.A. Hunter, R.J. Soto, M.H. Schoenfisch, S -Nitrosothiol-modified nitric oxide-releasing chitosan oligosaccharides as antibacterial agents, Acta Biomater. 12 (2015) 62–69. doi:10.1016/j.actbio.2014.10.028.
[16] V.F. Cardozo, C.A.C. Lancheros, A.M. Narciso, E.C.S. Valereto, R.K.T. Kobayashi, A.B. Seabra, G. Nakazato, Evaluation of antibacterial activity of nitric oxide-releasing polymeric particles against Staphylococcus aureus and Escherichia coli from bovine mastitis, Int. J. Pharm. 473 (2014) 20–29. doi:10.1016/j.ijpharm.2014.06.051.
[17] M.T. Pelegrino, L.C. Silva, C.M. Watashi, P.S. Haddad, T. Rodrigues, A.B. Seabra, Nitric oxide-releasing nanoparticles: synthesis, characterization, and cytotoxicity to tumorigenic cells, J. Nanoparticle Res. 19 (2017) 57. doi:10.1007/s11051-017-3747-4.
[18] L.S. Ferraz, C.M. Watashi, C. Colturato-Kido, M.T. Pelegrino, E.J. Paredes-Gamero, R.B. Weller, A.B. Seabra, T. Rodrigues, Antitumor potential of S -nitrosothiol-containing polymeric nanoparticles against melanoma, Mol. Pharm. 15 (2018) 1160–1168. doi:10.1021/acs.molpharmaceut.7b01001.
[19] A.B. Seabra, N.A. Kitice, M.T. Pelegrino, C.A.C. Lancheros, L.M. Yamauchi, P. Pinge-Filho, S.F. Yamada-Ogatta, Nitric oxide-releasing polymeric nanoparticles against Trypanosoma cruzi, J. Phys. Conf. Ser. 617 (2015) 12020. doi:10.1088/1742-6596/617/1/012020.
[20] C.A.C. Lancheros, M.T. Pelegrino, D. Kian, E.R. Tavares, P.M. Hiraiwa, S. Goldenberg, C.V. Nakamura, L.M. Yamauchi, P. Pinge-Filho, A.B. Seabra, S.F. Yamada-Ogatta, Selective antiprotozoal activity of nitric oxide-releasing chitosan nanoparticles against Trypanosoma cruzi: Toxicity and mechanisms of action, Curr. Pharm. Des. 24 (2018) 830–839. doi:10.2174/1381612824666180209105625.
[21] Q. Wang, Y. Zhao, L. Guan, Y. Zhang, Q. Dang, P. Dong, J. Li, X. Liang, Preparation of astaxanthin-loaded DNA/chitosan nanoparticles for improved cellular uptake and antioxidation capability, Food Chem. 227 (2017) 9–15. doi:10.1016/j.foodchem.2017.01.081.
[22] M. T. Pelegrino, A. B. Seabra, Chitosan-based nanomaterials for skin regeneration, AIMS Med. Sci. 4 (2017) 352–381. doi:10.3934/medsci.2017.3.352.
[23] K. Vig, A. Chaudhari, S. Tripathi, S. Dixit, R. Sahu, S. Pillai, V. Dennis, S. Singh, Advances in skin regeneration using tissue engineering, Int. J. Mol. Sci. 18 (2017) 789. doi:10.3390/ijms18040789.
[24] M. Pelegrino, B.A. Lima, M. do Nascimento, C. Lombello, M. Brocchi, A. Seabra, Biocompatible and antibacterial nitric oxide-releasing pluronic F-127/chitosan hydrogel for topical applications, Polymers (Basel). 10 (2018) 452. doi:10.3390/polym10040452.
[25] M.T. Pelegrino, D.R. de Araújo, A.B. Seabra, S-nitrosoglutathione-containing chitosan nanoparticles dispersed in Pluronic F-127 hydrogel: Potential uses in topical applications, J. Drug Deliv. Sci. Technol. 43 (2018) 211–220. doi:10.1016/j.jddst.2017.10.016.
[26] C.P. Bondonno, X. Yang, K.D. Croft, M.J. Considine, N.C. Ward, L. Rich, I.B. Puddey, E. Swinny, A. Mubarak, J.M. Hodgson, Flavonoid-rich apples and nitrate-rich spinach augment nitric oxide status and improve endothelial function in healthy men and women: a randomized controlled trial, Free Radic. Biol. Med. 52 (2012) 95–102. doi:10.1016/j.freeradbiomed.2011.09.028.
[27] P.M.C. Mommersteeg, R.G. Schoemaker, U.L.M. Eisel, I.M. Garrelds, C.G. Schalkwijk, W.J. Kop, Nitric oxide dysregulation in patients with heart failure, Psychosom. Med. 77 (2015) 292–302. doi:10.1097/PSY.0000000000000162.
[28] A.B. Seabra, M.G. de Oliveira, Poly(vinyl alcohol) and poly(vinyl pyrrolidone) blended films for local nitric oxide release, Biomaterials. 25 (2004) 3773–3782. doi:10.1016/j.biomaterials.2003.10.035.
[29] A.R. Butler, J.H. Ridd, Formation of nitric oxide from nitrous acid in ischemic tissue and skin, Nitric Oxide. 10 (2004) 20–24. doi:10.1016/j.niox.2004.01.004.
[30] C. Opländer, C.M. Volkmar, A. Paunel-Görgülü, E.E. van Faassen, C. Heiss, M. Kelm, D. Halmer, M. Mürtz, N. Pallua, C. V. Suschek, Whole body UVA irradiation lowers systemic blood pressure by release of nitric oxide from intracutaneous photolabile nitric oxide derivates, Circ. Res. 105 (2009) 1031–1040. doi:10.1161/CIRCRESAHA.109.207019.
[31] D.J. Sexton, A. Muruganandam, D.J. McKenney, B. Mutus, Visible light photochemical release of nitric oxide from s-nitrosoglutathione: potential photochemotherapeutic applications, Photochem. Photobiol. 59 (1994) 463–467. doi:10.1111/j.1751-

1097.1994.tb05065.x.
[32] J.B. Warren, Nitric oxide and human skin blood flow responses to acetylcholine and ultraviolet light., FASEB J. 8 (1994) 247–251. doi:10.1096/fasebj.8.2.7509761.
[33] S.M. Shishido, A.B. Seabra, W. Loh, M.G. de Oliveira, Thermal and photochemical nitric oxide release from S-nitrosothiols incorporated in Pluronic F127 gel: potential uses for local and controlled nitric oxide release, Biomaterials. 24 (2003) 3543–3553. doi:10.1016/S0142-9612(03)00153-4.
[34] A.N. Paunel, A. Dejam, S. Thelen, M. Kirsch, M. Horstjann, P. Gharini, M. Mürtz, M. Kelm, H. de Groot, V. Kolb-Bachofen, C. V. Suschek, Enzyme-independent nitric oxide formation during UVA challenge of human skin: characterization, molecular sources, and mechanisms, Free Radic. Biol. Med. 38 (2005) 606–615. doi:10.1016/j.freeradbiomed.2004.11.018.
[35] R. Weller, Nitric oxide: a key mediator in cutaneous physiology, Clin. Exp. Dermatol. 28 (2003) 511–514. doi:10.1046/j.1365-2230.2003.01365.x.
[36] R. Zuccarelli, A.C.P. Coelho, L.E.P. Peres, L. Freschi, Shedding light on NO homeostasis: Light as a key regulator of glutathione and nitric oxide metabolisms during seedling deetiolation, Nitric Oxide. 68 (2017) 77–90. doi:10.1016/j.niox.2017.01.006.
[37] A.R. Webb, H. Slaper, P. Koepke, A.W. Schmalwieser, Know your standard: Clarifying the CIE erythema action spectrum, Photochem. Photobiol. 87 (2011) 483–486. doi:10.1111/j.1751-1097.2010.00871.x.
[38] H. Jacobe, Treatment study comparing UVA-1 phototherapy vs placebo treatment for morphea, (2019). https://clinicaltrials.gov/ct2/show/NCT01799174 (accessed July 17, 2019).
[39] J.J. Voorhees, Ultraviolet (UVA and UVB) light therapy in the treatment of inflammatory skin conditions, (2019). https://clinicaltrials.gov/ct2/show/NCT00129415.
[40] A. Gęgotek, P. Domingues, E. Skrzydlewska, Proteins involved in the antioxidant and inflammatory response in rutin-treated human skin fibroblasts exposed to UVA or UVB irradiation, J. Dermatol. Sci. 90 (2018) 241–252. doi:10.1016/j.jdermsci.2018.02.002.
[41] P.C. Ford, I.M. Lorkovic, Mechanistic aspects of the reactions of nitric oxide with transition-metal complexes, Chem. Rev. 102 (2002) 993–1018. doi:10.1021/cr0000271.
[42] B.C. Smith, M.A. Marletta, Mechanisms of S-nitrosothiol formation and selectivity in nitric oxide signaling, Curr. Opin. Chem. Biol. 16 (2012) 498–506. doi:10.1016/j.cbpa.2012.10.016.
[43] S.L. Wynia-Smith, B.C. Smith, Nitrosothiol formation and S-nitrosation signaling through nitric oxide synthases, Nitric Oxide. 63 (2017) 52–60. doi:10.1016/j.niox.2016.10.001.
[44] A. Fraix, S. Sortino, Combination of PDT photosensitizers with NO photodononors, Photochem. Photobiol. Sci. 17 (2018) 1709–1727. doi:10.1039/C8PP00272J.
[45] C. Ratanatawanate, A. Chyao, K.J. Balkus, S- Nitrosocysteine-decorated PbS QDs/TiO2 nanotubes for enhanced production of singlet oxygen, J. Am. Chem. Soc. 133 (2011) 3492–3497. doi:10.1021/ja109328a.
[46] W. Yu, T. Liu, M. Zhang, Z. Wang, J. Ye, C.-X. Li, W. Liu, R. Li, J. Feng, X.-Z. Zhang, O2 economizer for inhibiting cell Respiration to combat the hypoxia obstacle in tumor treatments, ACS Nano. (2019). doi:10.1021/acsnano.8b07852.
[47] R.B. Weller, I love a sunburnt country: there's more to romance than cancer and vitamin D, Wound Rep Reg. 24 (2016) A13–A27.
[48] M.F. Holick, Biological effects of sunlight, ultraviolet radiation, visible light, infrared radiation and vitamin D for health, Anticancer Res. 36 (2016) 1345–1356. doi:0250-7005/2016 $2.00+.40.
[49] J. Dolanský, P. Henke, P. Kubát, A. Fraix, S. Sortino, J. Mosinger, Polystyrene nanofiber materials for visible-light-driven dual antibacterial action via simultaneous photogeneration of NO and O2 (1 Δ g), ACS Appl. Mater. Interfaces. 7 (2015) 22980–22989. doi:10.1021/acsami.5b06233.
[50] A. Fraix, O. Catanzano, I. Di Bari, C. Conte, M. Seggio, C. Parisi, A. Nostro, G. Ginestra, F. Quaglia, S. Sortino, Visible light-activatable multicargo microemulsions with bimodal photobactericidal action and dual colour fluorescence, J. Mater. Chem. B. 7 (2019) 5257–5264. doi:10.1039/C9TB00699K.
[51] N. V. Perricone, C.T. Madison, Systems and methods for treatment of acne vulgaris and other conditions with a topical nitric oxide delivery system, US 2014/0079761 A1, 2014.
[52] T. Münzel, A. Daiber, Inorganic nitrite and nitrate in cardiovascular therapy: A better alternative to organic nitrates as nitric oxide donors?, Vascul. Pharmacol. 102 (2018) 1–10. doi:10.1016/j.vph.2017.11.003.
[53] T. Münzel, A. Daiber, T. Gori, More answers to the still unresolved question of nitrate tolerance, Eur. Heart J. 34 (2013) 2666–2673. doi:10.1093/eurheartj/eht249.
[54] R. Zhang, D.T. Hess, J.D. Reynolds, J.S. Stamler, Hemoglobin S-nitrosylation plays an essential role in cardioprotection, J. Clin. Invest. 126 (2016) 4654–4658. doi:10.1172/JCI90425.
[55] B.K. Alba, J.L. Greaney, S.B. Ferguson, L.M. Alexander, Endothelial function is impaired in the cutaneous microcirculation of adults with psoriasis through reductions in nitric oxide-dependent vasodilation, Am. J. Physiol. Circ. Physiol. 314 (2018) H343–H349. doi:10.1152/ajpheart.00446.2017.

SUPPLEMENTARY DATA

This document presents supplementary data to the paper "Delivering nitric oxide into human skin from encapsulated S-nitrosoglutathione under UV light: an *in vitro* and *ex vivo* study". This supplementary file will be divided into sections accordingly with the paper chapters presented.

Summary

1. Materials and Methods

1.1. Chemicals

The pure chemicals used in this work where: Glutathione (GSH), sodium nitrite ($NaNO_2$), chitosan (CS, low molecular weight, 75 % of desacetylation), sodium tripolyphosphate (TPP), 5,5′-dithiobis (2-nitrobenzoic acid) (DTNB), ethylenediaminetetraacetic acid (EDTA), phosphate buffer (PBS), cupper chloride II ($CuCl_2$), and acetic acid. These chemicals were purchased from Sigma-Aldrich (St. Loius, MO, USA) ad used without

further purification. All experiments were carried out using high-purity water from a Millipore Milli-Q Gradient filtration system with resistivity not less than 18.2 MΩ·cm at 25.0 ºC.

1.2. Synthesis of GSNO

GSNO was synthesized by the nitrosation reaction of GSH. An aqueous solution of GSH (100 mmol·L^{-1}, pH 4.5) was mixed with an aqueous solution of $NaNO_2$ (100 mmol·L^{-1}, pH 4.5), at room temperature, for 5 min in the dark. The formation of GSNO was confirmed by recording the characteristic absorbance peak of GSNO at 336 nm (= 980.0 mol^{-1}·L·cm^{-1}), by using a plate reader (BioTek, Synergy HT, Vermont, USA) [1–3].

1.3. Synthesis of GSH-containing chitosan nanoparticles (GSH-CS NPs)

GSH-containing chitosan nanoparticles (GSH-CS NPs) were prepared by ionotropic gelation process [2,3]. In brief, aqueous solutions of CS (2.6 mg·mL^{-1}) and GSH (133.3 mmol·L^{-1}) were homogenized in 1 % acetic acid for 90 min, under magnetic stirring. An aqueous TPP solution (0.6 mg·mL^{-1}) was added dropwise to CS/GSH solution following the volumetric proportion of 3CS:1TPP. The final mixture was further stirred for 45 min at room temperature to leading to the formation of CS NPs (1000 µg of CS·mL^{-1}) containing GSH (100 mmol·L^{-1}). The GSH-CS NPs can be stored for at least 4 months.

1.4. Characterization of GSH-CS NPs

The synthesized GSH-CS NPs were characterized as described below.

1.4.1. Dynamic light scattering measurements (DLS)

The average hydrodynamic diameter (% by intensity), polydispersity index (PDI), and zeta potential of GSH-CS NPs were evaluated by DLS using a Nano ZS Zetasizer (Malvern Instruments Co, UK). The measurements were performed in three independent experiments at 25 °C using a fixed angle of 173° in disposable folded capillary zeta cells with a 10 mm path length in aqueous suspension.

1.4.2. GSH encapsulation efficiency into CS NPs

The encapsulation efficiency of GSH into CS NPs was measured by the quantification of free thiol groups using the Ellman's reagent [2,3]. To separate the free GSH molecules from encapsulated GSH, a volume of 500 µL of aqueous suspension of GSH-CS NPs was filtered in a Microcon centrifugal filter device (MWCO 10,000, Millipore). The eluted volume, containing non encapsulated GSH, was added to DTNB solution (0.7 mmol·L^{-1}) and EDTA (10.3 mmol·L^{-1}) at pH 7.4. After 5 min of incubation in the dark, the absorbance at 412 nm (ε = 14.15 $mmol^{-1}$·L·cm^{-1}) was measured in the UV-vis spectrophotometer Agilent 8454 (Palo Alto, CA, USA). The measurements were performed in duplicates.

1.4.3. Atomic force microscopy (AFM)

In order to investigate the shape and morphology of GSH-CS NPs, topography and phase contrast images were simultaneously obtained by atomic force microscope (AFM, AFM/SPM Series 5500, Agilent) in tapping mode. The free software *WSxM 5.0 Develop 8.2* was used to analyse the obtained images and plot the particle size histogram [4].

1.5. Nitrosation of GSH-CS NPs leading to the formation of GSNO-CS NPs

Free thiol group of GSH encapsulated in CS NPs was nitrosated, similar as described in section number1.2, leading to the formation of GSNO-containing CS NPs (GSNO-CS NPs) [2,3]. To this end, aqueous suspension of GSH-CS NPs (GSH concentration of 100 $mmol \cdot L^{-1}$, pH 4.5) was mixed with an aqueous solution of $NaNO_2$ (100 $mmol \cdot L^{-1}$, pH 4.5), at 5 – 8 ºC for 30 min in dark. The formation of GSNO into CS NPs was confirmed by detecting the characteristic absorbance peak of GSNO at 336 nm (= 980.0 $mol^{-1} \cdot L \cdot cm^{-1}$) using a plate reader (BioTek, Synergy HT, Vermont, USA) [1–3]. The GSNO-CS NPs should be immediately used after GSH nitrosation.

1.6. Monochromator

A single grating monochromator (model 77200, ThermoOriel, Newport, UK) with a 1000 W deuterium lamp was used to irradiate aqueous solutions and skin samples. The output light was attached to a liquid guide (5 mm diameter) to direct irradiate the samples. The wavelength calibration was conducted using a spectroradiometer (3AP-CAL, OphirOptronics Ltd, Jerusalem, Israel).

1.7. GSNO decomposition with NO release

The decomposition of free or encapsulated GSNO was measured by using UV-Visible spectrophotometric analysis. A volume of 2 mL of aqueous solution of free GSNO or aqueous suspension of GSNO-CS NPs (in both cases the initial GSNO concentration was 1.0 $mmol \cdot L^{-1}$) was transferred to a 12-well-plate. The plate was positioned under the light guide connected to monochromator, described in section number 1.6. The samples were irradiated using the liquid light guide with narrow wavelengths centered at 260, 270, 280, 290, 300, 310, 320, 330, 340, 360, 380 and 400 nm (precision of 0.1 nm). The samples were irradiated with different energies of 0-10 $J \cdot cm^{-2}$. The absorbance of GSNO was analyzed using the plate reader (*BioTek, Synergy HT, Vermont, USA*) by measuring the absorption intensity of GSNO at 336 nm. The decrease this absorption band intensity is associated with S-N bond cleavage of GSNO and free NO release [2,3]. The concentration of NO release over time was calculated from the amount of GSNO decomposed, through Equation 1and Equation 2.

$$[NO]_t = [GSNO]_0 - [GSNO]_t \quad \textit{Equation 1}$$

$$[NO]_t = (A_0 b)/\varepsilon_{GSNO} - (A_t b)/\varepsilon_{GSNO} \quad \textit{Equation 2}$$

Where $[NO]_t$ is NO concentration at time t, $[GSNO]_0$ and $[GSNO]_t$ are the concentrations of GSNO at the beginning of reaction and at time t, respectively; A_0 and A_t are the GSNO absorbance intensities at 336 nm at time zero and at time *t*, respectively; ε_{GSNO} is the molar absorption coefficient of GSNO at 336 nm; and b is the optical path of cuvette, which was normalized to 1.0 cm using the plate reader software.

The mathematical analysis for GSNO decomposition with NO release allowed to create contour maps showing the intensity of NO release, as a function of the selected wavelength. The NO release was determined by $[NO]_t$ acquired as a function of applied energy dose (ED), at a given wavelength. This mathematical procedure is described with more details in Supplementary Information section and the adjusted equations presented a determination coefficient (R^2) of no less than 0.96.

The free NO release analyses were collected using spectroscopy. This analysis reported the concentration of free NO in mmol·L^{-1}. For groups of (i) free GSNO (1.0 mmol·L^{-1}, pH 4.5), and (ii) GSNO-CS NPs (1.0 mmol·L^{-1}, pH 4.5), the concentration of free NO was acquired as a function of the applied energy dose (ED) at a given wavelength. This data showed that for a same wavelength the liberation of NO presents an initial linear growth and subsequent saturation at a given signal intensity ($[NO]_{max}$), as shown in Fig. 1-a. The equation in Fig. 1-b represents the Michaelis-Menten model and $[NO]_c$ stands for the calculated signal and ED_m for the energy dose in which $[NO] = [NO]_{max}/2$.

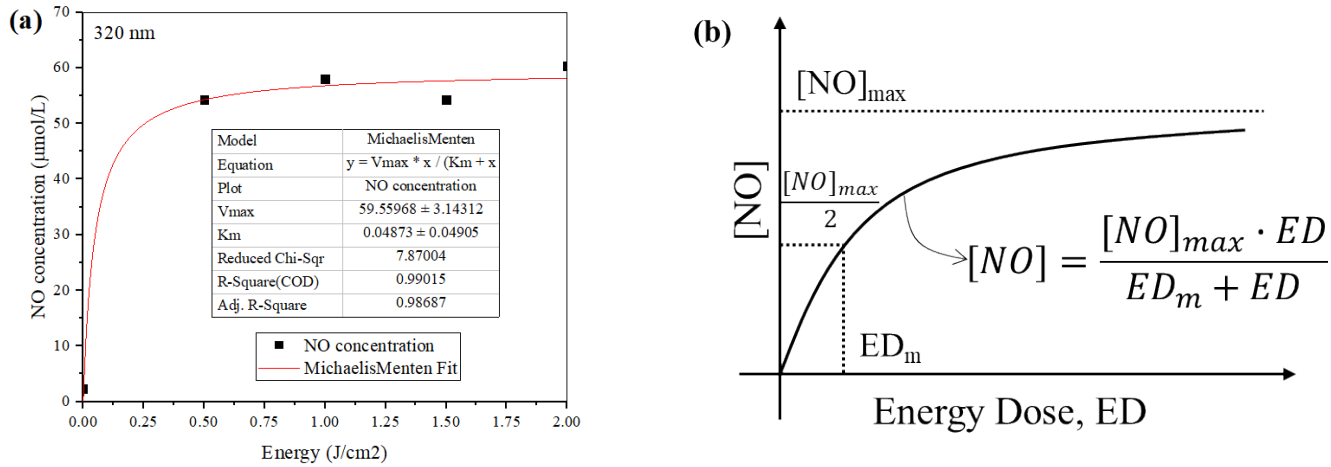

Fig. 1. (a) Collected and fitted data at 320nm and (b) schematic representations of the equation fitted.

The adjusted equations presented the determination coefficient (R^2) of no less than 0.96 presenting good fit to the data. As the focus of this study is to analyze the variation of NO production with light irradiation and not to quantify the amount of NO, the [NO] was normalized by dividing it by $[NO]_{max}$, and henceforth reported as $[NO]_n$ for each wavelength and calculated using for the energy dose interval from 0 to 10 J·cm^{-2} for every experimental sample group. This analysis allowed to create a contour maps showing the intensity of NO release

as a function of the wavelength of ultraviolet light irradiated for every NO forming chemical species analyzed. In addition, to evaluate the dose response of the irradiation in the NO release of the chemical species evaluated it was considered that until ED_m the curve of $[NO]_n$ versus ED presented linear behavior. By this consideration the angular coefficient is given by $([NO]_n/2)/ED_m$ and the angle between this line and the ED axis is given by the inverse tangent arc of this coefficient. By these considerations the NO response to dose (NO_{DR}) was calculated dividing the obtained angle by 90º so that if NO_{DR} approaches zero the response to the irradiation dose is null and if it approaches to one it is the maximum as possible for each chemical at a given wavelength, see Fig. 2.

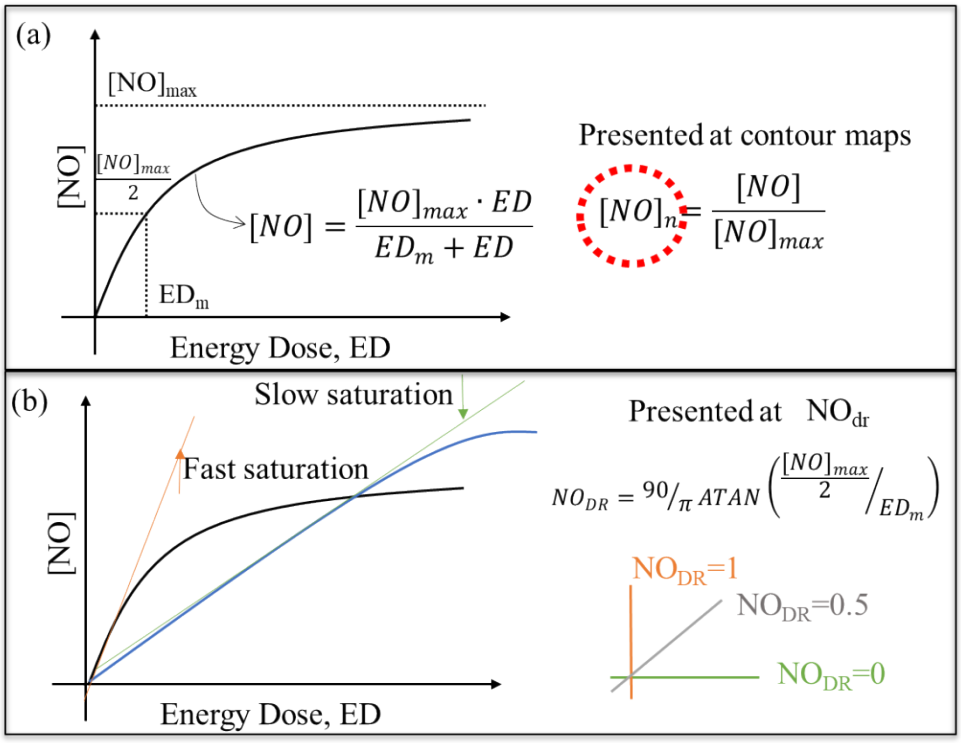

Fig. 2. Schematic representation of the calculation of (a) $[NO]_n$ and (b) NO_{DR}. Both are calculates at a constant wavelength

1.8. Human skin samples

Human skin samples were acquired from Murrayfield private hospital from abdominoplasty surgery (Edinburgh, Scotland, UK). After surgery, the skin slices were cleaned and transferred to Queen Medical Research Institute (QMRI) facility. The skin fat layer was removed using a scalpel and scissors. The skin was cut using dermatological punch with 4 mm of diameter and the skin slices were stored at - 20 ºC.

1.9. Free NO release from human skin slices pre-treated with GSNO-CS NPs

The amount of free NO release from untreated and treated human skin slices (4 mm) was measured. The pre-treatment consists in the incubation of skin slices with GSNO-CS NPs (GSNO concentration of 100.0

mmol·L^{-1}) for 2.5 h at 25 ºC in dark. After the incubation time, the skin samples were washed twice with Milli-Q water. Free NO release from treated and untreated skin slice was measured using the nitric oxide meter (ISO-NO, NOMK2, World Precision Instruments, WPI, FL, USA) with an electrochemical sensor (ISONOP-4 mm). To this end, 7 mL of Milli-Q water was transferred to a quartz cuvette (20 mm of optical path) containing treated or untreated skin slice. The electrochemical sensor was immersed into aqueous solutions (*ca*. 1 cm below top of quartz cuvette) and the signal of free NO production was electrochemically monitored, in dark and under irradiation. For the irradiation, the treated or untreated skin slices were irradiated using a liquid guide with narrow wavelengths centered at 280 and 320 nm (precision of 0.1 nm) at 3.0 J·cm^{-2}. The wavelengths were selected by using the monochromator, as described in the section 1.6.

1.10. Quantification of RSNO levels in human skin slices

The quantification of total RSNO contents in untreated and GSNO-CS NPs pre-treated human skin slices (4 mm) were determined. The pre-treatment consists in the incubation of human skin slices with GSNO-CS NPs (GSNO concentration of 100.0 mmol·L^{-1}) for 2.5 h at 25 ºC in dark. After the incubation time, the skin samples were washed twice with Milli-Q water. The skin samples were sub-divided in the following groups: (i) samples irradiated at 280 nm, (ii) samples irradiated at 320 nm, (iii) non-irradiated skin samples. The irradiation was performed by positioning the liquid guide on skin slices and applying wavelengths centered at 280 or 320 nm (precision of 0.1 nm) at 3.0 J·cm^{-2}. There were three replicates for each group (n=3). The wavelengths were selected by using the monochromator described in the section 1.6.

After the irradiation, the skin slices were homogenized using a glass tissue homogenizer of 15 cm^3 with 1.0 mL of Milli-Q water. After the homogenization, the samples were transferred to Eppendorf flasks and kept in an ice bath, in the dark. The levels of RSNOs generated in the skin were quantified by using the NO meter (*ISO-NO, NOMK2, World Precision Instruments, WPI, FL, USA*) with an electrochemical NO sensor (ISONOP-4 mm). To this end, an aqueous solution of copper chloride was used to allow the quantification of NO release from RSNO, as previously described (Oliveira et al., 2016; Silveira et al., 2016). The NO sensor was immersed in a solution of 10 mL of copper chloride II ($CuCl_2$) at 0.1 mol·L^{-1}. A volume of 200 µL of skin homogenate supernatant was added to the $CuCl_2$ solution. The experiments were performed in duplicates of two independent experiments (n=4) and the calibration curves were obtained with aqueous solutions of freshly prepared GSNO (data not shown) [5].

1.11. Statistical analysis

Data are presented as mean values ± standard error of the mean (SEM). Statistical analysis was performed using Origin Pro 2016 software by one-way ANOVA followed by Tukey post-test. Differences were considered statistically significant when $p < 0.05$.

2. Results

CS NPs have been used in different applications such as drug delivery system, tissue engineering and as antimicrobial agent [6–9]. The wide range of biomedical applications of CS NPs are intrinsically related to CS properties, such as antimicrobial effects, mucoadhesiveness, biodegradability and biocompatibility [7,8]. Firstly, GSH molecule, the precursor molecule of the NO donor, was encapsulated into CS NPs, followed by its nitrosation leading to formation of GSNO-containing CS NPs.

GSH-CS NPs have a hydrodynamic size of 123.3 ± 1.5 nm, with a moderate polydispersity of 0.25 ± 0.01, and a positive zeta potential of + 25.0 ± 1.1 mV, as characterized by DLS. These findings are in agreement with previous reports that show the formation of CS NPs for the encapsulation of different molecules (5-fluoracil, insulin, and mercaptossunic acid)[10–13]. The particles are in the nanometer scale in aqueous medium with moderate polydispersity, which are desirable for biomedical applications [10]. The positive value of zeta potential is related to the presence of protonated amino groups in CS chemical structure and its magnitude indicates a good stability of the colloidal suspension of CS NPs [3,10,13].

The encapsulation efficiency (EE%) of GSH into CS NPs was found to be 99.6 %. The interaction of protonated amino groups in CS chemical structure with carboxyl groups in GSH and phosphate groups in TPP contributed to the high encapsulation efficiency observed for GSH into CS NPs [12,14]. This result is in accordance with our previous reports [2,3,12]. Moreover, Ali & Ahmed, 2018 showed an EE % of 88 and 90 % for protein and SiRNA encapsulated into CS NPs, respectively [15,16].

Fig. 3-a shows a representative AFM image of GSH-CS NPs. It can be observed a spherical shape of the nanoparticles with a good dispersion at solid state. Fig. 3-b shows the diameter size histogram of GSH-CS NPs, in which the average size was estimated to be 28.86 ± 3.30 nm. This size corresponds to average size of CS NPs at solid state, and it is in accordance with previously reported data. For instance, Zhang et al. reported an average size of 40 nm at solid state for CS NPs containing polyphenol [6] (Zhang & Zhao, 2015), and Tzeyung et al. reported an average size of 20 nm for CS NPs containing rotigotine, a drug used for the treatment of Parkinson´s disease [17].

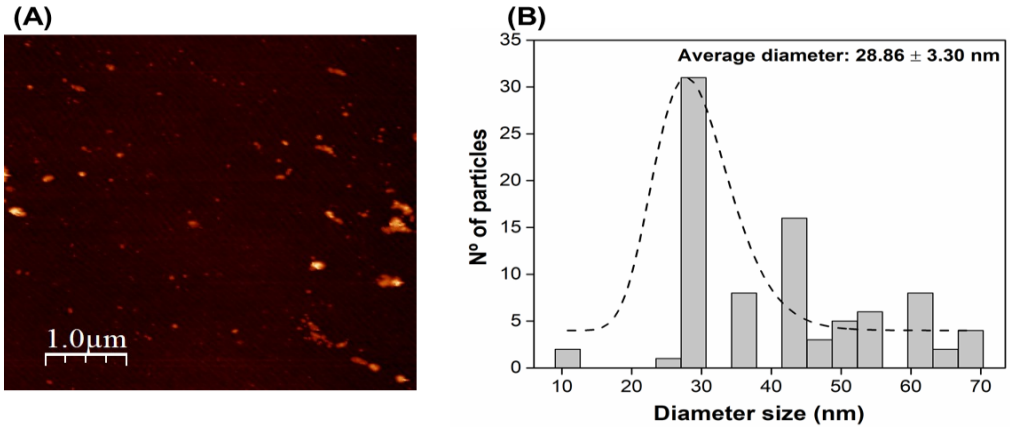

Fig. 3. (A) Representative atomic force microscopy (AFM) topography image and (B) diameter size histogram with a fitted log-normal curve (dotted black line) for GSH-CS NPs (GSH concentration of 100.0 mmol·L-1)

It should be noted that the average size of nanoparticles at solid state is expected to be lower compared to nanoparticle hydrodynamic size[3,18], assayed by DLS measurements, in agreement with data reported herein. Therefore, GSH-CS NPs were successful synthesized with a size distribution, polydispersity and shape suitable for biomedical applications [19].

Free thiol group of GSH incorporated into CS NPs was nitrosated by reacting with an equimolar amount of $NaNO_2$, in slightly acidic aqueous suspension. $NaNO_2$ in acid aqueous suspension is dissociate into Na^+ and NO_2^- ions and it can generate the nitrous acid (HNO_2), responsible for the thiol nitrosation, as represented in Equation 3. This reaction leads to formation of GSNO encapsulated into CS NPs. The formation of GSNO into CS NPs was confirmed by the detection of an absorption band at 336 nm, assigned to S-NO group (Figure 2). The absorption band at 336 nm was observed for GSNO-CS NPs, and absence for GSH-CS NPs, as expected (Figure 2).

$$GSH + HNO_2 \rightarrow GSNO + H_2O \qquad \textit{Equation 3}$$

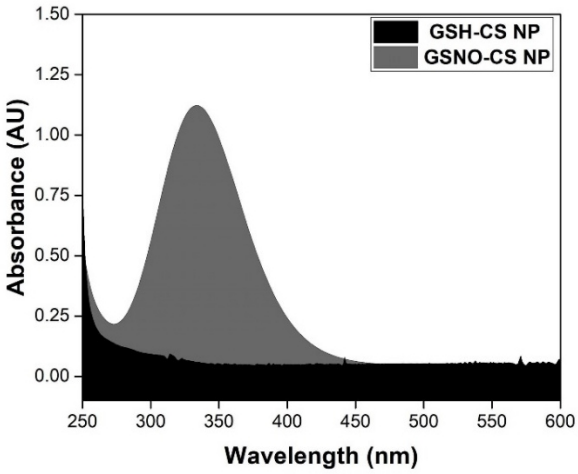

Fig. 4. Uv spectra of GSH-CS NPs and GSNO-CS NPs. The absorption band at 336 nm confirms the formation of S-NO groups

Fig. 5 shows the CS NPs absorbance UV-vis spectrum. The CS NPs absorbs light around 200-300 nm. The amplitude decrease of NO generation after GSNO encapsulation into CS NPs is related to CS NPs absorbance of light in this range.

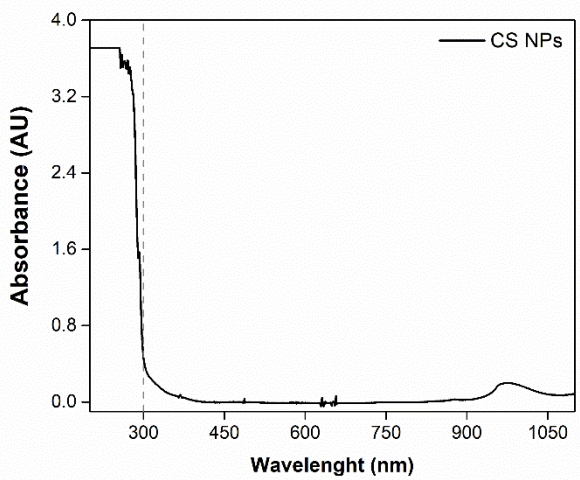

Fig. 5. Absorbance spectrum of CS NPs.

3. References

[1] N.M. Silveira, L. Frungillo, F.C.C. Marcos, M.T. Pelegrino, M.T. Miranda, A.B. Seabra, I. Salgado, E.C. Machado, R. V. Ribeiro, Exogenous nitric oxide improves sugarcane growth and photosynthesis under water deficit, Planta. 244 (2016) 181–190. doi:10.1007/s00425-016-2501-y.

[2] M.T. Pelegrino, R.B. Weller, X. Chen, J.S. Bernardes, A.B. Seabra, Chitosan nanoparticles for nitric oxide delivery in human skin, Med Chem Comm. 8 (2017) 713–719. doi:10.1039/C6MD00502K.

[3] M.T. Pelegrino, L.C. Silva, C.M. Watashi, P.S. Haddad, T. Rodrigues, A.B. Seabra, Nitric oxide-releasing nanoparticles: synthesis, characterization, and cytotoxicity to tumorigenic cells, J. Nanoparticle Res. 19 (2017) 57. doi:10.1007/s11051-017-3747-4.

[4] I. Horcas, R. Fernández, J.M. Gómez-Rodríguez, J. Colchero, J. Gómez-Herrero, A.M. Baro, WSXM: A software for scanning probe microscopy and a tool for nanotechnology, Rev. Sci. Instrum. 78 (2007) 13705. doi:10.1063/1.2432410.

[5] H.C. Oliveira, B.C.R. Gomes, M.T. Pelegrino, A.B. Seabra, Nitric oxide-releasing chitosan nanoparticles alleviate the effects of salt stress in maize plants, Nitric Oxide. 61 (2016) 10–19. doi:10.1016/j.niox.2016.09.010.

[6] H. Zhang, Y. Zhao, Preparation, characterization and evaluation of tea polyphenol–Zn complex loaded β-chitosan nanoparticles, Food Hydrocoll. 48 (2015) 260–273. doi:10.1016/j.foodhyd.2015.02.015.

[7] K. Divya, S. Vijayan, T.K. George, M.S. Jisha, Antimicrobial properties of chitosan nanoparticles: Mode of action and factors affecting activity, Fibers Polym. 18 (2017) 221–230. doi:10.1007/s12221-017-6690-1.

[8] A. Anitha, N. Deepa, K.P. Chennazhi, S.V. Nair, H. Tamura, R. Jayakumar, Development of mucoadhesive thiolated chitosan nanoparticles for biomedical applications, Carbohydr. Polym. 83 (2011) 66–73. doi:10.1016/j.carbpol.2010.07.028.

[9] C.A.C. Lancheros, M.T. Pelegrino, D. Kian, E.R. Tavares, P.M. Hiraiwa, S. Goldenberg, C.V. Nakamura, L.M. Yamauchi, P. Pinge-Filho, A.B. Seabra, S.F. Yamada-Ogatta, Selective antiprotozoal activity of nitric oxide-releasing chitosan nanoparticles against Trypanosoma cruzi: Toxicity and mechanisms of action, Curr. Pharm. Des. 24 (2018) 830–839. doi:10.2174/1381612824666180209105625.

[10] M.A. Elgadir, M.S. Uddin, S. Ferdosh, A. Adam, A.J.K. Chowdhury, M.Z.I. Sarker, Impact of chitosan composites and chitosan nanoparticle composites on various drug delivery systems: A review, J. Food Drug Anal. 23 (2015) 619–629. doi:10.1016/j.jfda.2014.10.008.

[11] A.B. Seabra, N.A. Kitice, M.T. Pelegrino, C.A.C. Lancheros, L.M. Yamauchi, P. Pinge-Filho, S.F. Yamada-Ogatta, Nitric oxide-releasing polymeric nanoparticles against Trypanosoma cruzi, J. Phys. Conf. Ser. 617 (2015) 12020. doi:10.1088/1742-6596/617/1/012020.

[12] M. Pelegrino, B.A. Lima, M. do Nascimento, C. Lombello, M. Brocchi, A. Seabra, Biocompatible and antibacterial nitric oxide-releasing pluronic F-127/chitosan hydrogel for topical applications, Polymers (Basel). 10 (2018) 452. doi:10.3390/polym10040452.

[13] L.S. Ferraz, C.M. Watashi, C. Colturato-Kido, M.T. Pelegrino, E.J. Paredes-Gamero, R.B. Weller, A.B. Seabra, T. Rodrigues, Antitumor potential of S -nitrosothiol-containing polymeric nanoparticles against melanoma, Mol. Pharm. 15 (2018) 1160–1168. doi:10.1021/acs.molpharmaceut.7b01001.

[14] R.V. Kumaraswamy, S. Kumari, R.C. Choudhary, A. Pal, R. Raliya, P. Biswas, V. Saharan, Engineered chitosan based nanomaterials: Bioactivities, mechanisms and perspectives in plant protection and growth, Int. J. Biol. Macromol. 113 (2018) 494–506. doi:10.1016/j.ijbiomac.2018.02.130.

[15] H. Katas, M.A.G. Raja, K.L. Lam, Development of Chitosan Nanoparticles as a Stable Drug Delivery System for Protein/siRNA, Int. J. Biomater. 2013 (2013) 1–9. doi:10.1155/2013/146320.

[16] A. Ali, S. Ahmed, A review on chitosan and its nanocomposites in drug delivery, Int. J. Biol. Macromol. 109 (2018) 273–286.

doi:10.1016/j.ijbiomac.2017.12.078.
[17] A. Tzeyung, S. Md, S. Bhattamisra, T. Madheswaran, N. Alhakamy, H. Aldawsari, A. Radhakrishnan, Fabrication, optimization, and evaluation of rotigotine-loaded chitosan nanoparticles for nose-to-brain delivery, Pharmaceutics. 11 (2019) 26. doi:10.3390/pharmaceutics11010026.
[18] W.R. Rolim, M.T. Pelegrino, B. de Araújo Lima, L.S. Ferraz, F.N. Costa, J.S. Bernardes, T. Rodigues, M. Brocchi, A.B. Seabra, Green tea extract mediated biogenic synthesis of silver nanoparticles: Characterization, cytotoxicity evaluation and antibacterial activity, Appl. Surf. Sci. 463 (2019) 66–74. doi:10.1016/j.apsusc.2018.08.203.
[19] M. T. Pelegrino, A. B. Seabra, Chitosan-based nanomaterials for skin regeneration, AIMS Med. Sci. 4 (2017) 352–381. doi:10.3934/medsci.2017.3.352.